EVALUATION OF STRENGTH AND DURABILITY PROPERTIES OF CEMENTITIOUS COMPOSITES WITH RICE STUBBLE BIOCHAR AS PARTIAL BINDER REPLACEMENT

A Thesis report submitted in the partial fulfilment for the award of the degree of
MASTER OF ENGINEERING
In
STRUCTURAL ENGINEERING

Submitted by
PARSHANT KUMAR
Registration No. 802324008

Under the Guidance of

Dr. Danie Roy A.B.
Associate Professor
Department of Civil Engineering
TIET, Patiala

Dr. Arpit Goyal
General Manager
Cathodic Protection Group
Structural Specialities & Projects (India)

THAPAR INSTITUTE
OF ENGINEERING & TECHNOLOGY
(Deemed to be University)

DEPARTMENT OF CIVIL ENGINEERING

THAPAR INSTITUTE OF ENGINEERING AND TECHNOLOGY
PATIALA

DECEMBER 2025

CERTIFICATE

This is to certify that the thesis titled "**EVALUATION OF STRENGTH AND DURABILITY PROPERTIES OF CEMENTITIOUS COMPOSITES WITH RICE STUBBLE BIOCHAR AS PARTIAL BINDER REPLACEMENT**", submitted by ***Parshant Kumar*** (***Registration number: 802324008***), as a part of the curriculum of **Master of Engineering** program in Structural Engineering specialization in the **Department of Civil Engineering** at **Thapar Institute of Engineering and Technology**, is a record of the candidate's original and independent work carried out under our supervision and guidance. The matter presented in this thesis report has not been submitted previously, in part or full, at any other Institution for the award of any degree in India or abroad.

Dr. Danie Roy A.B.
Associate Professor
Department of Civil Engineering
TIET
Patiala

Dr. Arpit Goyal
General Manager
Cathodic Protection Group
Structural Specialities & Projects (India)

DECLARATION

I, ***Parshant Kumar***, hereby declare that this work titled "**EVALUATION OF STRENGTH AND DURABILITY PROPERTIES OF CEMENTITIOUS COMPOSITES WITH RICE STUBBLE BIOCHAR AS PARTIAL BINDER REPLACEMENT**" submitted as a partial requirement for the completion of **Master of Engineering** program is the record of my own independent work conducted under the supervision of ***Dr. Danie Roy A.B***. and ***Dr. Arpit Goyal***. References to the work by other researchers and other existing literature are duly listed. The matter presented in this thesis report has not been submitted previously, in part or full, at any other Institution for the award of any degree in India or abroad.

Parshant Kumar.

Parshant Kumar

ACKNOWLEDGEMENT

I wish to express my deepest and most sincere gratitude and appreciation for my supervisors, ***Dr. Danie Roy A.B.*** and ***Dr. Arpit Goyal***, for their continued guidance, support and patience. I truly feel fortunate to have had them as my supervisors and am indebted to them for their patience and understanding. I can never find words good enough to express my deep and sincere gratitude to them. I wish to emulate their patience and kindness.

I also wish to thank postgraduate co-ordinator, ***Dr. Himanshu Chawla*** for his patience, support and encouragement. I wish to thank my seniors and Doctoral research scholars, ***Dr. Akshay Sharma*** and ***Mr. Sarmad Rashid,*** for their kind support, encouragement and guidance throughout this process. They stepped up to assist me in all matters and motivated me throughout. I am deeply grateful. I am also indebted to ***Mr. Abhishek Chandel,*** Doctoral research scholar, Department of Physics and Material Science and ***Mr. Tanveer Singh Jhajj ,*** Doctoral research scholar, Department of Energy and Environment, for their support, friendship and guidance**.**

I would also like to thank the staff of the Structural Engineering Laboratory, specifically Mr Varinder Kumar Sharma, Mr Atul Pandey, Mr Amit Thakur, and Mr Ram Sumiran, for their assistance and support throughout the experimental program.

I want to thank the staff at Nava Nalanda Central Library, particularly ***Ms. Archana Nanda*** for their extraordinary support and stepping up to assist me by providing otherwise inaccessible publications.

Most importantly, I am grateful to my parents and my wife for their constant support and love. Your sacrifices, love and unconditional support has been my guiding light and I can never repay this debt of gratitude.

And lastly, my alma mater, or as the latins thought of it, the *"nourishing mother"*, ***Thapar Institute of Engineering and Technology***, the place I called home for a very long time. Thank you for everything.

With a heart full of gratitude.

Parshant Kumar

ABSTRACT

This study examines the impact of varying proportions of biochar produced from the pyrolysis of rice stubble waste on the strength and durability performance of cementitious composites. Ordinary Portland cement was partially replaced with finely ground biochar at replacement levels of 0%, 2.5%, 5%, 7.5%, and 10%. The resulting concrete mixes were prepared, cast, and cured under controlled conditions. The primary objective was to determine the optimal biochar dosage and evaluate the influence of biochar incorporation on fresh, mechanical, and durability characteristics of concrete through slump test, rebound hammer test, ultrasonic pulse velocity test, compressive strength test, splitting tensile strength test, flexural strength test, water absorption test, and rapid chloride permeability test.

It was observed that increasing biochar concentration led to a progressive reduction in slump, indicating stiffer mixes due to the high porosity and water absorption capacity of the biochar particles. Compressive strength testing revealed that incorporating biochar enhanced the compressive strength, with a 7.5% replacement dosage emerging as the optimal dosage. However, higher dosages still yielded improved strengths relative to the control mix. In contrast, splitting tensile and flexural strengths decreased with increasing biochar content, attributed to the internal porosity introduced within the concrete matrix.

Rebound hammer results exhibited agreement with the compressive strength trends, while ultrasonic pulse velocity outcomes similarly confirmed that M-3 (7.5% biochar) exhibited the highest pulse velocity, corresponding to its superior compressive strength. Rapid chloride permeability results further validated the enhanced performance of M-3, which demonstrated the lowest charge passed, indicating reduced chloride ion penetration. Conversely, water absorption showed an increasing trend with biochar content, with M-4 presenting the highest absorption value.

Overall, it can be concluded that M-3, containing 7.5% biochar as partial cement replacement, represents the optimum mix composition, while higher dosages still provide improvements over the control mix in several aspects. This study highlights that incorporating biochar can promote matrix densification due to its fine particle size and filler effect; however, it may simultaneously increase overall porosity when introduced beyond the optimum dosage threshold.

TABLE OF CONTENTS

LIST OF TABLES

LIST OF FIGURES

LIST OF ABBREVIATIONS

IPCC	Intergovernmental Panel on Climate Change
NET	Negative Emission Technology
C-S-H	Calcium silicate hydrate
HTC	Hydrothermal carbonization
LWAs	Light-weight aggregates
LWAC	Lightweight aggregate concrete
BC	Biochar
MPa	Mega-Pascal
TRHB	Treated rice husk biochar
TBB	Treated bagasse biochar
FWD	Food waste digestate
ASTM	American Society for Testing and Materials
BIS	Bureau of Indian Standards
OPC	Ordinary Portland Cement
PCE	Polycarboxylic ether
HR-WRA	High-range water reducing admixture
UTM	Universal testing machine
UPV	Ultrasonic pulse velocity
RCPT	Rapid chloride permeability test
XRD	X-ray diffraction
SEM	Scanning electron microscopy/microscope
FE-SEM	Field emission Scanning electron microscopy/microscope
EDS	Energy dispersive spectroscopy
ACI	American Concrete Institute

CHAPTER 1
INTRODUCTION

1.1 Overview

Concrete and its primary binder, cement, are the central focus of global infrastructure development, as they constitute the most essential construction materials in modern society. With the construction industry expanding rapidly worldwide, particularly across emerging economies, the demand for concrete and cement has reached unprecedented levels. Concrete is the second most utilized material on the planet, surpassed only by water. As global urbanization accelerates, so does the associated environmental burden. According to the 2017 report of the Global Alliance for Buildings and Construction, infrastructure and building activities contribute nearly 40% of energy-related CO_2 emissions. These emissions have steadily increased over the last decades. As reported by the International Energy Agency (2021), worldwide anthropogenic CO_2 emissions reached 31.5 gigatonnes in 2020. Moreover, research by Habert et al. (2020) estimates that cement production alone accounts for approximately 36% of the CO_2 generated by the construction sector, and nearly 8% of all human-related CO_2 emissions globally. The increasing concentration of atmospheric CO_2 represents one of the most serious threats to environmental stability, potentially triggering severe climatic consequences.

Since the natural carbon cycle is now insufficient to reabsorb these anthropogenic emissions, urgent measures are required to actively capture and store CO_2 from industrial processes such as construction. Among the possible solutions, the identification and utilization of waste-derived supplementary materials for partial cement replacement have emerged as promising and widely researched strategies for reducing the environmental footprint of concrete.

1.2 Biochar as a potential solution

The Intergovernmental Panel on Climate Change (IPCC, 2018) has recognized biochar as an important Negative Emission Technology (NET). The incorporation of biochar into construction materials—either as partial cement replacement or as aggregate modification shows strong potential due to its unique physical characteristics and sustainability benefits. Biochar is a carbon-rich product derived from thermal decomposition of biomass under

oxygen-deficient conditions. Its porous structure and high specific surface area allow it to absorb and sequester CO_2 from the surrounding environment. Studies have shown that biochar may possess a carbon footprint of approximately −2 to −3.3 kg CO_2 equivalent per kg of biochar, depending upon the source biomass. It is estimated that even a modest addition of 1 kg of biochar to concrete can capture and store up to 2.5 kg of CO_2. Globally, around 140 gigatonnes of biomass waste are produced annually. If 373 million tonnes of biochar could be produced, it may sequester up to 500 million tonnes of CO_2 annually equivalent to roughly 1.5% of global emissions (*Windeatt et al., 2014*).

1.3 Positive effects of Biochar- A brief overview

Extensive research has indicated that biochar exhibits chemical and physical compatibility with the cementitious matrix due to its high porosity and reactive surface properties. For instance, a 2019 study titled Utilization of biochars from sugarcane bagasse pyrolysis in cement-based composites by Rodier et al. reported a 9% increase in cement hydration when 2% biochar was introduced into the mixture. Other notable studies, such as the "Strength and durability improvements of biochar-blended mortar or paste using accelerated carbonation curing" by Yang and Wang, and "Accelerated carbonation of hardened cement pastes: Influence of porosity" by Wang et al., concluded that biochar incorporation enhances cement hydration, decreases permeability, and improves chloride resistance. Additionally, research by Zanotto et al. documented lower oxygen ingress in biochar-enhanced concrete, thereby reducing risks of reinforcement corrosion. Therefore, concrete containing biochar not only contributes to long-term atmospheric carbon immobilization but also facilitates the use of agricultural waste, offering a dual environmental benefit absent in conventional concrete.

1.4 Properties of Biochar that influence Concrete Performance

Pore structure: Micro-pore networks serve as reservoirs for fluid retention within the concrete mixture, assisting in internal moisture regulation and potentially improving curing efficiency.
Particle size and distribution: Finely divided biochar particles enhance packing density by filling interstitial voids between cement grains, resulting in a denser and stronger concrete matrix.
Surface area: The extremely high surface area of biochar promotes pozzolanic reactivity. During hydration, calcium hydroxide reacts with biochar-borne aluminosilicates to produce

additional C–S–H gel, thereby improving strength and durability while enabling reduced cement consumption.

1.5 Factors affecting the properties of biochar

Properties of biochar vary widely depending on its production parameters. Temperature of pyrolysis, thermal ramp rate, residence time, source biomass, and environmental pressure conditions significantly influence characteristics such as pore volume, surface area, and water retention behaviour (*Malajaee et al., 2021*). These variations ultimately affect workability and engineering performance when used in concrete.

1.6 Types of Biochar Production Processes

Biochar may be produced from diverse biomass sources agricultural residue, forestry waste, food scraps, sewage sludge, and municipal solid wastes. The major production approaches include pyrolysis, gasification, hydrothermal carbonization (HTC), torrefaction, and co-pyrolysis. Each technique yields biochars with distinct microstructural properties, resulting in variations in concrete behaviour.

1.6.1 Pyrolysis Biochar

Conventional pyrolysis typically at temperatures between 400–1200°C remains the most widely used biochar production method due to its cost-effectiveness. Different variants such as slow, fast, flash, and vacuum pyrolysis produce biochars with distinct pore networks and surface areas.

1.6.2 Gasification Biochar

Gasification converts biomass primarily into hydrogen-rich syngas at elevated temperatures (700–1500°C). The residual char exhibits significantly developed pore structures and potentially superior performance in concrete, owing to its higher internal curing capacity and accelerated carbonation effects.

1.6.3 Hydrothermal Carbonization Biochar (Hydrochar)

HTC processes wet biomass without pre-drying, thereby conserving energy. However, hydrochar may contain undesirable compounds, such as heavy metals and hydrocarbons, necessitating thorough purification before its use in structural applications.

1.6.4 Torrefaction

Conducted at 200–300°C in oxygen-free conditions, torrefaction yields biochar with reduced ash and sulfur content, thus offering lower combustion-related emissions.

1.6.5 Co-pyrolysis

Multiple biomass varieties are thermally decomposed together, producing hybridized biochar compositions with mixed properties.

1.7 Methods of Biochar replacement in cementitious composites

Biochar can be introduced directly as a substitute for cement or as a filler. However, such application introduces challenges such as increased absorption and dust-handling hazards. Alternatively, biochar can be processed into lightweight aggregate pellets using either conventional sintering or cold bonding. Cold-bonded biochar aggregates exhibit mechanical performance comparable to that of sintered aggregates, but with drastically reduced CO_2 emissions, offering the potential for highly sustainable, low-weight concretes.

1.8 Research gaps

Despite numerous studies demonstrating the potential mechanical and environmental benefits of biochar in cementitious systems, there remain several unresolved research gaps:

- Most studies are limited to biochar derived from specific biomass sources; limited research exists on biochar sourced from rice stubble, despite India producing large quantities of this waste annually.

- There is insufficient clarity regarding the optimal dosage of biochar for balanced mechanical and durability performance, particularly beyond 5%.
- Only a few studies systematically correlate fresh properties (e.g., slump) with mechanical behaviours (compressive, tensile, flexural) and durability aspects (chloride resistance, water absorption) in a unified experimental framework.
- Limited research exists on long-term durability performance of biochar concrete, particularly relating to permeability, internal pore structure, and carbonation behaviour. This thesis specifically addresses these gaps by investigating biochar derived from rice stubble at multiple replacement levels, with detailed characterization of both mechanical and durability properties.

1.9 Objectives of the present study

The objectives of this research are:

1. To use biochar made from pyrolysis of rice-stubble waste as partial binder replacement at varying dosages and evaluate its influence on the workability of cementitious composites.
2. To assess the influence of biochar addition on the mechanical properties of concrete, at different curing ages.
3. To assess durability indicators of biochar-incorporated concrete.

CHAPTER 2
LITERATURE REVIEW

This chapter synthesizes the existing body of research related to the incorporation of biochar and other lightweight aggregates in cementitious systems. The review highlights how biochar, when used in various forms, affects the physical, mechanical, and durability properties of concrete, as well as its broader environmental implications. As the scientific interest in carbon-sequestering construction materials has grown significantly in recent years, a detailed examination of prior studies is necessary to understand the current state of knowledge, methodological approaches, and limitations in the field. The literature reviewed in this chapter encompasses experimental investigations, comparative analyses, and theoretical studies that examine the impact of biochar and other lightweight aggregate materials on concrete performance under various dosage levels, production conditions, and replacement strategies. In particular, research findings on workability, hydration mechanisms, compressive and tensile behaviour, permeability, carbonation potential, and structural applicability have been examined to establish a foundation for the present study.

Based on the reviewed literature, biochar and other lightweight aggregates have typically been incorporated into concrete in three principal forms: first, as a partial replacement for cement, where finely ground biochar functions as a pozzolanic additive or micro-filler; second, as a substitute for natural sand or coarse aggregates, replacing traditional mineral aggregates to modify density and internal pore structure; and third, as engineered bonded lightweight aggregates, in which biochar is pelletized or chemically bonded with stabilizing agents to create synthetic aggregate particles used in lightweight aggregate concrete (LWAC). Through this examination of prior studies, the research critically evaluates both the advantages and limitations of these approaches, identifies areas requiring further exploration—particularly with respect to biochar derived from rice stubble residues and establishes the contextual foundation for how the present study aims to expand knowledge in the field of sustainable cementitious materials.

2.1. Cement replacement

2.1.1 Compressive Strength

Gupta et al. (2018) conducted an investigation the effect of biochar in mortar mix when used as a cement replacement. Four types of mixes were produced, out of which two were control mixes, one with a water-cement ratio of 0.40 (Control 1) and the other with water-cement ratio of 0.35 (Control 2). The other two mixes had 2% (by weight of cement) biochar added to the mix, one with saturated biochar (CO_2 saturated BC) and the other being Unsaturated biochar added (no CO2 adsorbed in the pores). It was observed that 28 days compressive strength of mortar with saturated biochar added and that with unsaturated biochar added were 34.20 MPa and 40.92 MPa, as opposed to 38 MPa for Control 1. It was also observed that at 7 days curing age, there was a significant improvement in the compressive strength with the addition of both saturated and unsaturated biochars. This was attributed to micro-filler effect shown by biochar, which contributes in accelerated hydration and causes a denser matrix.

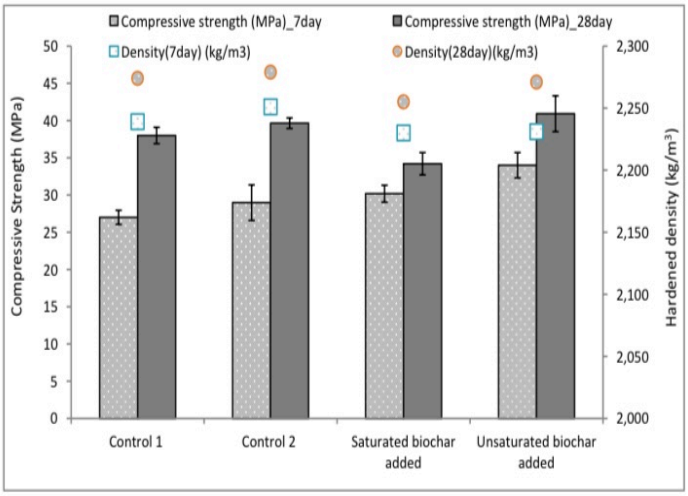

Figure 2.1 Density and Compressive strength of the samples (Gupta and Kua, 2018)

Gupta et al. (2020) conducted a study focused on studying the effect of biochar being used as a partial replacement of cement and silica fume. In this study, three types of biochars were used, namely SWBC, TBC and CBC. SWBC was produced as a result of wood wastes being shredded to wood chips 3-4 cm in size and then dried to 80 °C, finally being pyrolyzed at 500 °C for 1 hour in steady state. TBC was a commercial grade biochar procured as-is. This was also originally prepared from the pyrolysis of wood waste at 105 °C for 24 hours. CBC was the coconut shell biochar produced by treating the untreated coconut biochar (CBC-UT) was

further ground and reheated to get CBC. D_{50} CBC, TBC, SWBC were 8 µm, 5 µm and 4 µm respectively. Whereas, D_{50} for Portland cement and silica fume were 33 µm and 5 µm. It was observed that 7 days compressive strengths of CBC5, TBC5 and SWBC5 were almost similar to that of the plain mortar. This showed that up to 5% weight of cement can be substituted with biochar without any adverse effect on compressive strength. At 28 days age, SF15 (control 2) showed higher strength as compared to Control 1 by about 19%. It was also observed that carbon rich BC (TBC and CBC in this case) caused higher strength development than BC with high oxygen (ash) content i.e. SWBC. Increase in CH content from 7 to 28 days was observed to be only about 2.5% in plain cement paste but 27.5% in TBC5, signifying positive impact of TBC in promoting hydration. Similarly, CBC5 showed a 12.8% increase in CH content from 7 to 28 days. Interestingly, CBC5SF10 and TBC5SF10 showed very similar 28 days compressive strength as that of SF15 (control 2).

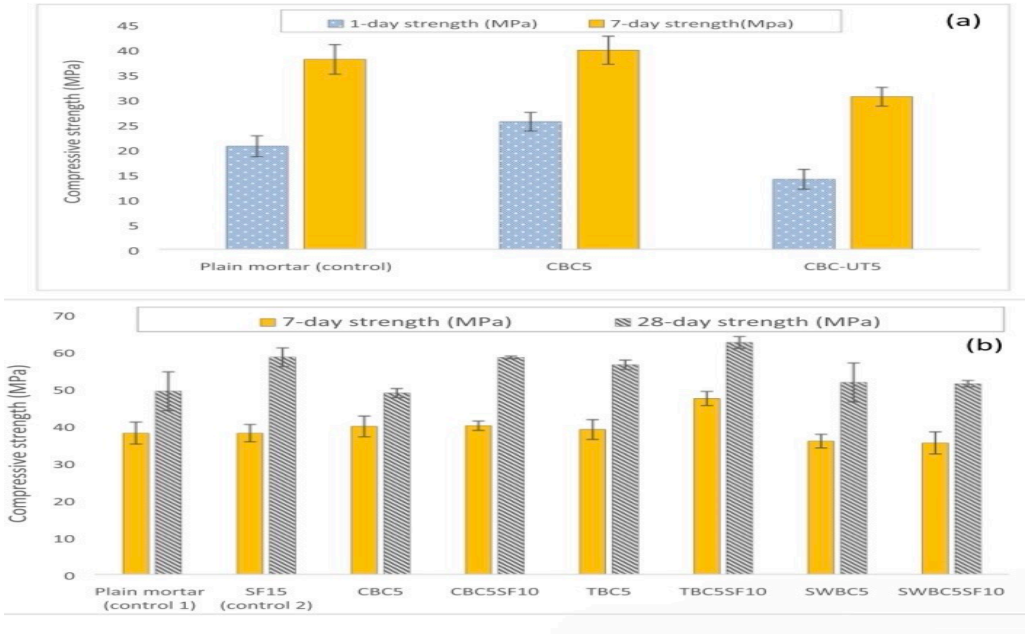

Figure 2.2 Compressive strengths of BC mortars at 1, 7 and 28 days (Gupta et al. 2020)

Liu et al. (2022) studied the effect of replacement of cement with the bamboo biochar, pyrolyzed at 650 ◦C for a residence time of 25 minutes. Majority of BC particles were in the size range of 50 to 80 µm and were predominantly of regular shape. Water-cement ratio was kept at 0.8 for all the mixes and Bamboo biochar replaced the cement at 0%, 0.2%, 0.4%, 1%, 2%, 3% and 4% by weight leading to Control, BC0.2, BC0.4, BC1, BC2, BC3 and BC4 mixes, respectively. It was noticed that early strength development increased with increase in biochar dosage. 7 days strength of the mixes were 58.2%, 62.7%, 61.2%, 61%, 66.7%, 69.9% and

72.2% of the 40 days compressive strength, for the mixes ranging from control to BC4 respectively. This can be attributed to the fact that biochar particles absorbed water at early age hence decreasing the water-cement ratio, producing high early strength. Subsequently, this adsorbed water was released at later stages, thus enhancing the hydration process. It was also noted that with respect to the control group, strength development at 7 days age were 8.5%, 9.6%, 22%, 29.3%, 30.5% and 32.9% respectively. This is because of the filler effect of small biochar particles. Interestingly and contrastingly, at 14 days age, compressive strength increased for 1% BC replacement but decreased for higher dosages. This was explained with the fact that the hydration products of bamboo biochar are less than. Calcium silicate hydrate formed overall, therefore replaced biochar contributing to the hydration but not as much as that of cement hydration. Additionally, biochar introduces higher porosity to biochar mixes. Hence, it can be concluded that bamboo biochar introduced compressive strength enhancement in the mixes, w.r.t the control mix. 1% dosage by weight had the peak strengthening effect, whereas 1% to 4% replacements led to positive improvements.

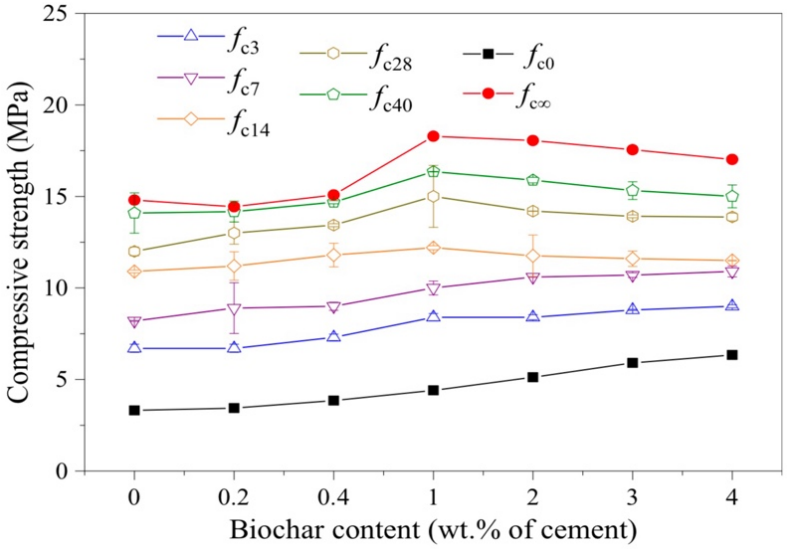

Figure 2.3 Compressive strengths of the mixes with varying BC dosages (Liu et al. 2022)

Sikora et al (2022) conducted study on the effect of addition of wood chip biochar used as cement replacement. Ordinary Portland Cement was replaced by biochar at 0%,2%, 5%, 10%, 15% and 20% respectively for mixes B0, B2, B5, B10, B15 and B20. Additionally, cement mortar mixes were also prepared, namely BM0, BM2, BM5, BM10 and BM20. It was reported that BM2 and BM5 showed 2% and 3% higher compressive strength than reference., while BM10 had a compressive strength 4% lower than BM0. Further, BM20 had a further decrease of 29% in its compressive strength, w.r.t BM0. Similarly, in the case of cement pastes, 28 days

compressive strength of the mixes containing BC was lower than that of the reference mix (B0). B2, B5, B10, B15 and B20 had 7%, 12%, 21%, 23% and 35% lower compressive strength than B0, respectively. It is noteworthy that irrespective of the dosage of biochar, the compressive strength decreased because the biochar particles in this study were coarser than the cement particles, since D50 and D90 of biochar being 22 μm and 74 μm. Therefore, a more porous matrix were generated.

Roy et al. (2017) conducted a research in which biochar was used as cement replacement. This biochar was produced as a result of pyrolyzing the poultry litter and enhanced poultry litter (with bentonite added to it) at 450℃. Six mixes were prepared, three each with Poultry litter biochar and enhanced poultry litter biochar, where the biochars were used to replace cement at 0%, 1%, 5% and 10% replacement %. Expectedly, the compressive strength of all the samples with EPL Biochars were greater than that of PL Biochars. It was observed that compressive strength decreased with increasing biochar dosage. However all the samples had compressive strength greater than 12.5 MPa, which is the minimum required compressive strength for mortar to be used in structural applications, as per standard guidelines laid down in CCANZ (2010): New Zealand concrete masonry manual.

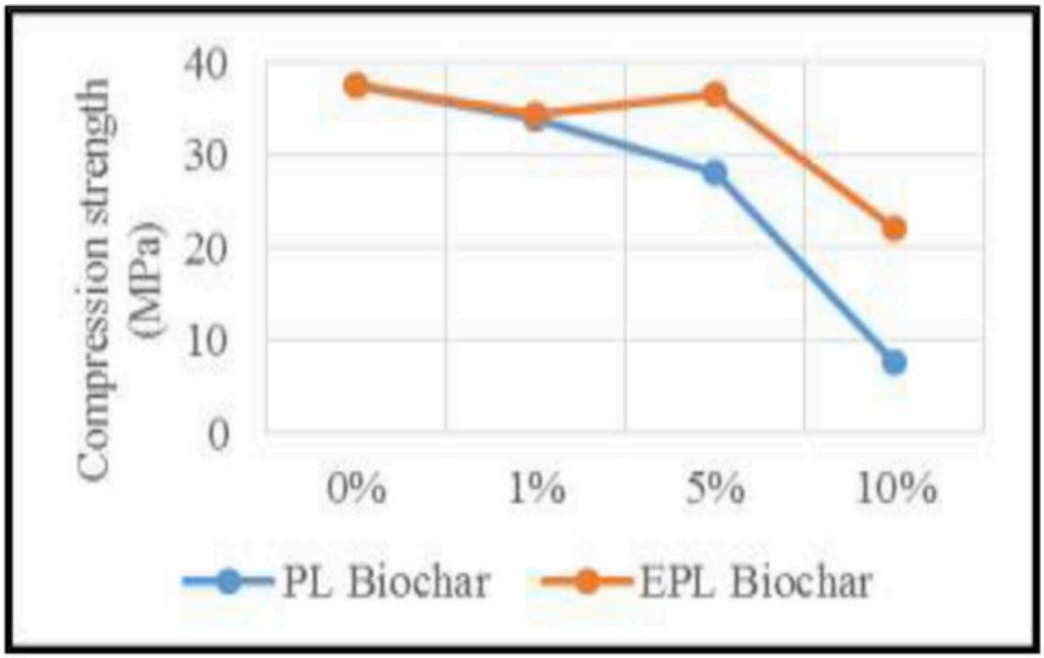

Figure 2.4 Compressive strengths of poultry litter and enhanced poultry litter BC mixes

(Roy et al. 2017)

2.1.2 Flexural Strength

Jia et al. (2023) studied the effect of partial replacement of cement with biochar prepared by pyrolyzing Municipal Solid Waste at 600 ◦C. Three mix designs were prepared, i.e. C40, C30 and C20 with compressive strengths of 40, 30 and 20 MPa respectively. Further, each of these mixes were added with 1, 2, 3. 4, 5, 10, 20 and 30% by weight of MSW BC as cement replacement, resulting in 27 mixes in total. It was found that addition of 3% MSW BC as cement replacement in C-40 Mix led to 8.5% improvement in flexural strength. At 30% replacement level, the flexural strengths of C-40, C-30 and C-20 dropped to 3.4, 2.8 and 2.7 MPa, which was a loss of 27.4%, 21.5% and 24.5%, respectively.

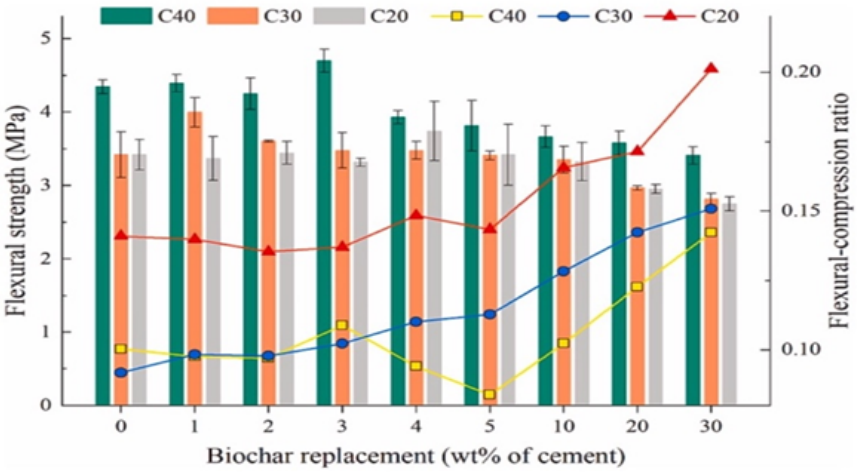

Figure 2.5 Flexural strengths of mixes containing MSW Biochar in different dosages (Jia et al. 2023)

Ling et. al (2023) studied the effects of biochar as a cement replacement on flexural strength and other properties. Waste wood biomass was pyrolyzed at 500 ◦C and then crushed in pulverizer for different durations to obtain four different types of biochars with different fineness, i.e. BC-1, BC-2, BC-3 and BC-4 with fineness of 44.70 μm, 73.28 μm, 750 μm and 1020 μm, respectively. These biochars were then added in the mixes as cement replacement at 0%, 1%, 3%, 5% and 10% by weight and a constant water-binder ratio of 0.45. It was observed that at 1% and 3% dosage, flexural strength increased marginally, while for higher dosages (5% and above), flexural strength was lower than that of control group. This decreasing trend was increasingly prominent with increasing dosage and fineness. 28 days' flexural strength of BC-4 concrete, having 10% cement by weight replaced by biochar and maximum fineness was

about 78% of the flexural strength of control mix. Similarly, flexural strength of BC-1, having 10% cement by weight replaced by biochar and minimum fineness, had flexural strength about 80% that of control group.

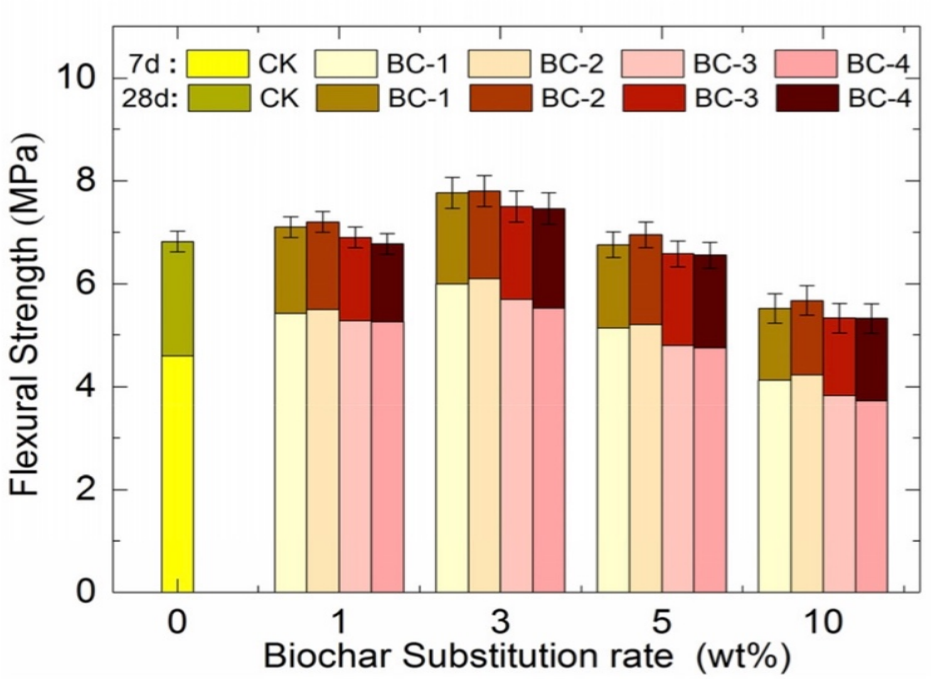

Figure 2.6 Flexural strengths at different biochar replacement levels (Wu et al. 2023)

Du et al. (2023) studied the effect of two types of biochars used at cement replacement on shrinkage and other properties. Fresh biochar was produced by pyrolysing vetiver grass roots at 500 °C. Additionally, used biochar was produced by soaking fresh biochar in water with rich concentrations of Cd, Pb, Zn and Cu, simulating the leaching of heavy metals. In total, nine mixes were produced including one control mix with no biochar, and four mixes each with fresh and used biochars, with 0.5%, 1%, 1.5% and 2% biochar by weight added as cement replacement. Maximum flexural strength was observed for the mix with 1% biochar dosage, which was 28.7 MPa for fresh biochar replacement and 27.8 MPa for used biochar substitution, which were 20% and 16% improvements over control mix for fresh and used biochar, respectively. It was observed, as expected, that compared to the fresh biochar, addition of used biochar decreased the flexural performance overall. In both the cases of fresh and used biochars, addition of dosage higher than 1% decreased the flexural performance. For example, 28 days flexural strengths for mixes with 2% fresh and used biochars were 11% and 14% lower than the control mix, respectively.

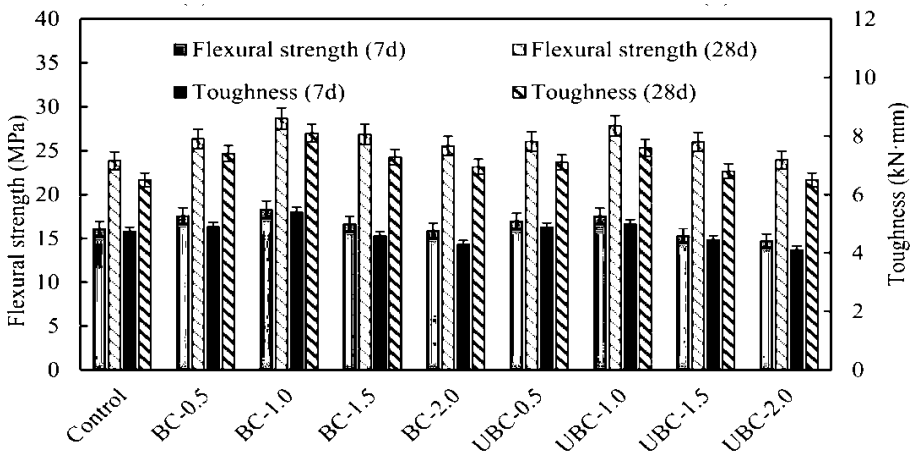

Figure 2.7 Flexural properties of UHPC Mixes with varying biochar dosage (Du et al. 2023)

2.1.3 Splitting Tensile Strength

Jia et al. (2023) studied the effect of partial replacement of cement with biochar prepared by pyrolyzing Municipal Solid Waste at 600 ◦C. Three mix designs were prepared, i.e. C40, C30 and C20 with compressive strengths of 40, 30 and 20 MPa respectively. Further, each of these mixes were added with 1, 2, 3. 4, 5, 10, 20 and 30% by weight of MSW BC as cement replacement, resulting in 27 mixes in total, with a constant water-cement ratio of 0.45. It was observed that addition of 2% BC improved splitting tensile strength by 10.6% w.r.t the reference mix. Higher dosages, beyond 2% caused reduction in the tensile strength. It was observed that the effect of MSW BC was not as pronounced on splitting tensile strength as it was on the compressive strength. This could be because of low elastic modulus of biochar.

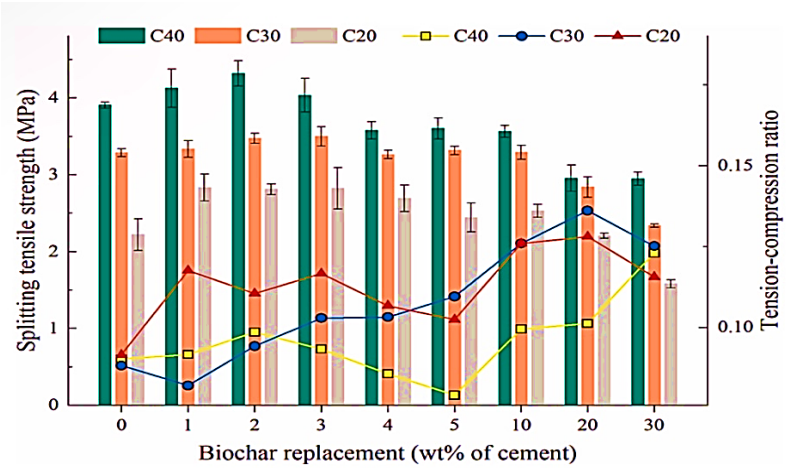

Figure 2.8 Splitting tensile strengths of mixes with varied dosages of MSW-BC (Jia et al. 2023)

Zeidabadi et al. (2018) studied the effect of addition of biochar as cement replacement on the properties of the mixes. Three types of biochars were produced by the pyrolysis at 700 °C for a residence time of 2 hours, i.e. treated rice husk biochar (TRHB), unpretreated rice husk biochar (RHB), pretreated bagasse biochar (TBB) and unpretreated bagasse biochar (BB). Biochars were used to replace cement in cement pastes at 0%, 5% and 10% replacement levels. Water-cement ratio of 0.5 was adopted throughout. It was observed, overall, addition of all types of biochars led to increase in the tensile strength w.r.t the mix with no biochars. Replacing 5% cement with treated and untreated rice husk biochar improved the tensile strength of the mixes. At the same time, 10% cement replacement with treated bagasse biochar and treated rice husk biochar resulted in reduction of the tensile strength.

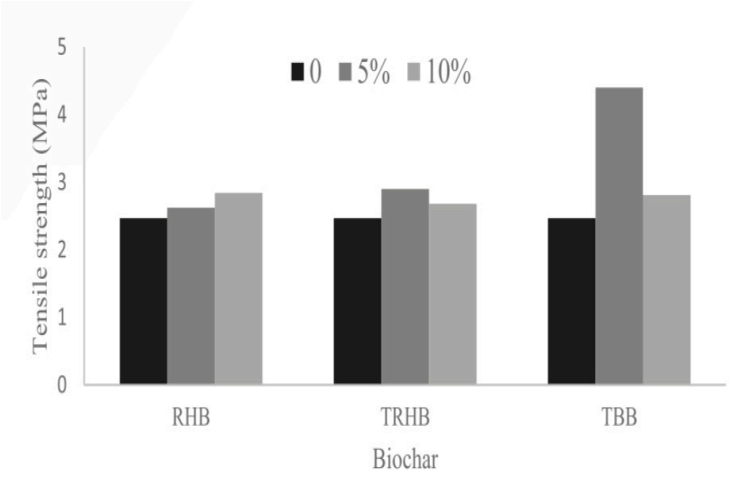

Figure 2.9 Tensile strength of the mixes with rice husk and bagasse biochar (Zeidabadi et al. 2018)

2.1.4 Shrinkage

Gupta et al. (2020) observed that as far as the autogenous shrinkage is concerned, At 91 days, a very significant decrease of about 42% and 51% was observed in CBC5 and SWBC5 w.r.t the control. At 91 days age, TBC5 exhibited higher autogenous shrinkage than CBC5 and SWBC5, about 72% higher than CBC5 and double that of SWBC5, even though all three had comparable porosity and pore surface area. While at 28 days, TBC5 showed 88% and 200% higher autogenous shrinkage than CBC5 and SWBC5. With the addition of 15% silica fume, autogenous shrinkage increased by 81% and 29% at 28 and 91 days respectively. It was also observed that at 28 days, CBC5SF10, TBC5SF10 and SWBC5SF10 had autogenous reduced by 63%, 23% and 77% respectively. Hence, it was clear that combination of silica fume and biochar reduced shrinkage strain significantly, hence reducing the extent of micro-cracking due

to self-desiccation. This is due to the fact that biochar acts as internal curing agent due to its moisture retention capacity, releasing moisture as a consequence and preventing self-desiccation. In context to the total shrinkage, while CBC5 and TBC5 showed comparable shrinkage strain at 91 days, SWBC5 had a marginal decrease of 11% in total shrinkage, in reference to plain mortar. Similar to the sealed (autogenous) shrinkage, TBC5 showed higher total shrinkage 7-28 days phase, which was followed by a decrease in shrinkage. At 91 days, 15% addition of silica fume enhanced total shrinkage by about 24% w.r.t plain mortar. Whereas, a 33% replacement of silica fume with biochar reduced total shrinkage by 16%, 12% and 23% for CBC5SF10, TBC5SF10 and SWBC5SF10 respectively, w.r.t SF15.

Du et al. (2023) studied the effect of two types of biochars used at cement replacement on shrinkage and other properties. Fresh biochar was the product of the pyrolysis of vetiver grass roots at 500 ◦C. Additionally, used biochar was produced by soaking fresh biochar in water with rich concentrations of Cd, Pb, Zn and Cu, simulating the leaching of heavy metals. In total, nine mixes were produced including one control mix with no biochar, and four mixes each with fresh and used biochars, with 0.5%, 1%, 1.5% and 2% biochar by weight added as cement replacement. It was observed that at 28 days age, autogenous shrinkage decreased from 821 με to 742 με, at 2% cement replacement with fresh biochar, while the corresponding reduction in the case of the addition of used biochar was from 821 με to 717 με. This trend was because of the fact that presaturated biochar acted as internal curing agent, consequently diminishing the shrinkage. Additionally, lead ions in used biochar decreased the shrinkage.

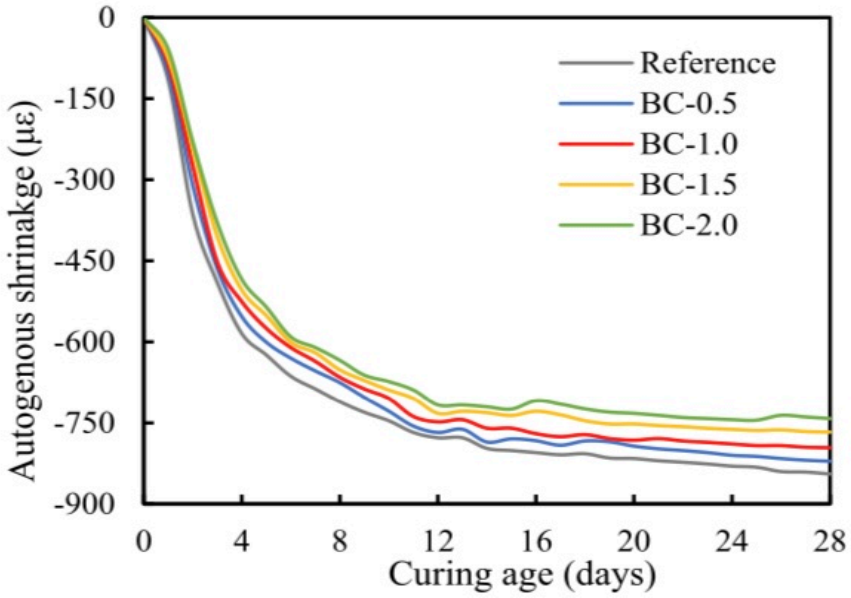

Figure 2.10 Autogenous shrinkage of UHPC with varied dosages of fresh biochar (Du et al. 2023)

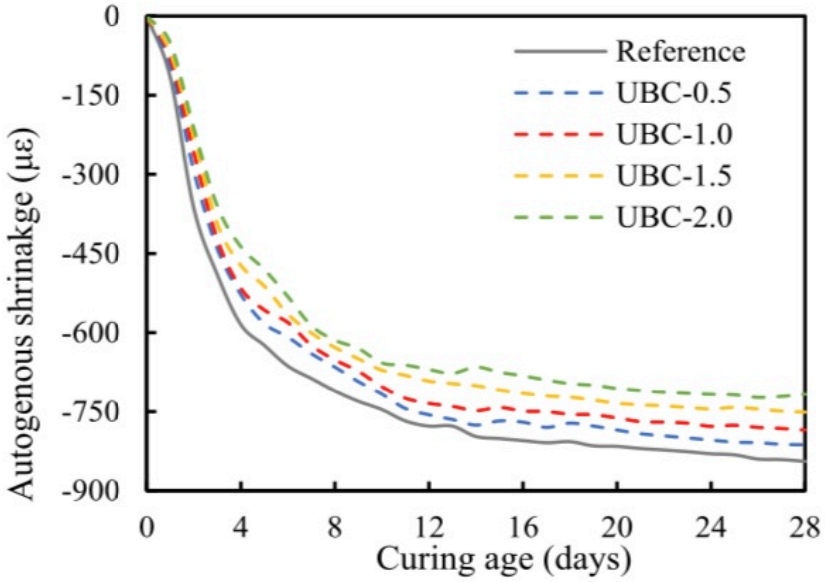

Figure 2.11 Autogenous shrinkage results of UHPC mixes with different dosages of used biochar (Du et al. 2023)

2.1.5 Water absorption

Gupta et al. (2020) conducted another study focused on studying the effect of biochar being used as a partial replacement of cement and silica fume. In this study, three types of biochars were used, namely SWBC, TBC and CBC. SWBC was produced as a result of wood wastes being shredded to wood chips 3-4 cm in size and then dried to 80 °C, finally being pyrolysed at 500 °C for 1 hour in steady state. TBC was a commercial grade biochar procured as-is. This was also originally prepared from the pyrolysis of wood waste at 105 °C for 24 hours. CBC was the coconut shell biochar produced by treating the untreated coconut biochar (CBC-UT) was further ground and reheated to get CBC. CBC, TBC, SWBC were 8 μm, 5 μm and 4 μm respectively. Whereas, D_{50} for Portland cement and silica fume were 33 μm and 5 μm. It was observed that CBC5, TBC5 and SWBC5 had reduced water absorption w.r.t plain mortar, with decrement ranging between 12 and 17%. This reduction in water absorption is due to the filler effect of biochar particles as well as enhanced hydration rate attributed to the internal curing effect. Another observation was that CBC5, TBC5 and SWBC5 mixes had 28%, 29% and 38% lesser initial sorptivity w.r.t the plain mortar, respectively. This was due to the pore refinement of bulk matrix and the ITZs due to the addition of the biochars. At the same time, CBC5 exhibited a secondary sorptivity 80%, 76% and 73% lower than the plain mortar, TBC5 and SWBC5, respectively. This lower secondary sorptivity of CBC5 w.r.t the other two 5% dosage BC Mixes, i.e. TBC5 and SWBC5 was due to the greater pore tortuosity and lower permeability

of CBC, as compared to TBC and SWBC. One more major observation was that SF15 had 75% less initial sorptivity than the control, owing to the pozzolanic effect and filler action of silica fume. A related and similar trend was seen in the mixes with combination of both silica fume and biochar. It was seen that CBC5SF10, TBC5SF10 and SWBC5SF10 had higher CH content than SF15.

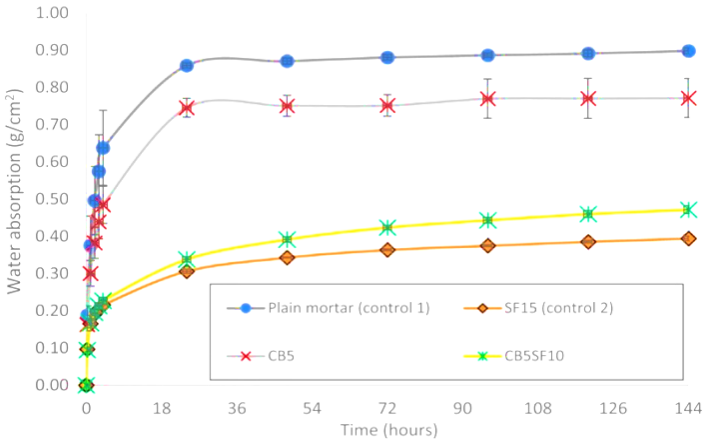

Figure 2.12 Water absorption of mixes with coconut BC and biochar- Silica Fume combination (Gupta et al. 2020)

Roy et al. (2017) conducted a research in which biochar was used as cement replacement. This biochar was produced as a result of pyrolyzing the poultry litter and enhanced poultry litter (with bentonite added to it) at 450℃. Six mixes were prepared, three each with Poultry litter biochar and enhanced poultry litter biochar, were the biochars were used to replace cement at 0%, 1% , 5% and 10% replacement %. Samples prepared underwent water curing for 7 and 28 days. Water absorption testing was done as per ASTM C642 to quantify the water retention capacity of 75 × 75 × 250 mm samples which were cured for 28 days. It was observed that biochar mixes had higher water absorption than the control mix. At 10% addition by volume, water absorption of the mortar almost doubled, attributed to high water retention capacity of biochar. It was also observed that poultry litter biochar and enhanced poultry litter biochar resulted in almost comparable influence on the water absorption of the mortar mixes.

2.1.6 CO_2 Sequestration and emissions

Tang and Qiu et. al (2024) lightweight concretes were developed using reactive magnesia cement, Sodium hexametaphosphate, NWAs (micro-silica sand, mean particle size 150 mu-m), very high amount of LWAs (BC or shale particles both finer than 1 mm, up to 61 vol% of

concrete). Biochar was developed by the pyrolysis of peanut shells at 500 ◦C. For Mixes 0 to 160, RMC-to-biochar varied from 0 to 1.6. Water-cement ratio adopted was 0.79. Separately, S100 Mix was made with RMC, Silica sand, Oven dried Shales (instead of Biochar) and water as a reference (or control) to B100. It was seen that Biochar mixes sequestered CO_2 Using two methods: (i) CO_2 fixating chemically to hydrated cement through its carbonation process: and (ii) CO_2 being physically adsorbed by biochar's surface.

2.2 Filler/ Aggregate replacement

2.2.1 Compressive Strength

Praneeth et al. (2021) In this study, enhanced poultry litter was pyrolyzed to form biochar which was used as a filler material, as a replacement of sand, and its effect on the mixes was studied. Sand was replaced in the range of 10% to 40% of the total weight. Four mixes were prepared: B-0, B-10, B-20 and B-40 corresponding to 0, 10,20 and 40% BC dosages, respectively. Water cement ratio used was 1:2.5 and water-binder ratio was 0.5. Average particles sizes in this study were Cement: 8.05 µm, sand: 311.75 µm and Biochar: 26 µm. There was a marked decreasing trend in the compressive strengths of the mixes with increasing biochar dosage. Biggest reduction in compressive strength took place in the case of B-10, w.r.t B-10, which experienced a 21% decrease in compressive strength. This decrease in the compressive strength was explained as the fact that due to very high dosages of biochar in concrete, the volume of the pores of biochar is greater than the volume of the hydration products formed in these pores, hence making a more porous matrix as opposed to denser ones in the case of relatively lower biochar dosages.

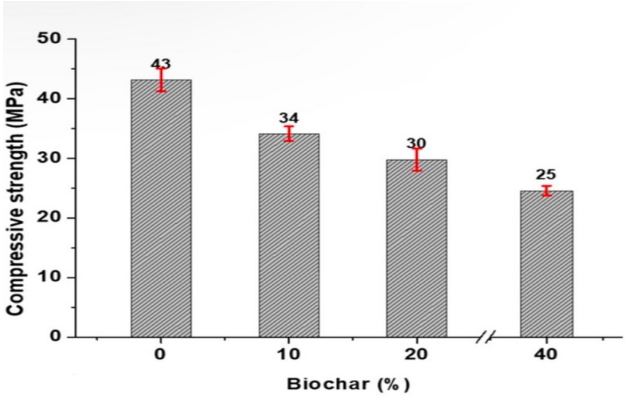

Figure 2.13 Compressive strength of mixes with varied BC dosage (Praneeth et al. 2021)

Chen et al. (2024) studied the effect of food waste digestate biochar used as aggregate replacement on compressive strength and other properties of the mixes. Three types of biochars were made from food waste digestate corresponding to three different temperatures, i.e. FWD550BC, FWD650BC and FWD750BC produced at 550°C, 650°C and 750°C, respectively. Three mixes were produced i.e. FWD550BC, FWD650BC and FWD750BC in the form of cubic blocks. In this study, filler and aggregate were completely absent and only biochar is used as filler. Biochar also served as internal curing agent, which means water could be stored in its pores and then released and used to enhance hydration of cement. As a result, water demand for hydration is less than that of concretes and mortars with no biochar in it. 28 days Compressive strength of FWD550BC, FWD650 and FWD750 mixes were 48.5, 52.7 and 57.8 MPa, respectively. Evidently, biochars with higher porosity, i.e. FWD650BC and FWD750BC caused improved compressive strengths, w.r.t FWD550BC. The increase in compressive strength increased with higher pyrolysis temperature.

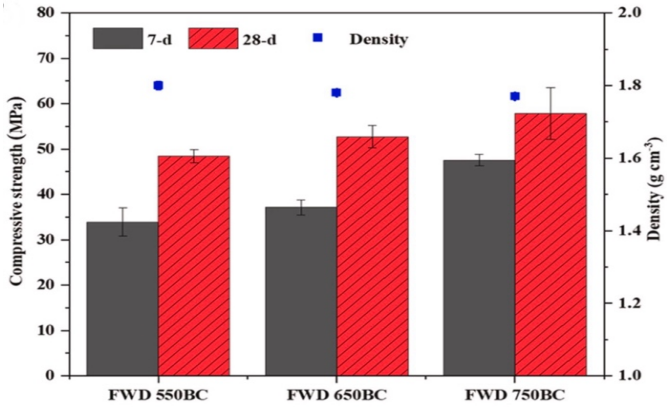

Figure 2.14 Compressive strengths of mixes with different types of biochar (Chen et al. 2024)

Besides compressive strengths higher than 40 MPa, indicating that LWAC can be used for high strength applications, it was also observed that density of all FWD Biochar blocks were less than 2 g cm^{-3}, indicating that all the mixes qualified as Light weight mixes, as per the standards laid by ACI 213R-03 (Guide for structural Lightweight-Aggregate Concrete).

Maljaee et al. (2022) studied the effect of replacing olive stone waste biochar as a replacement of coarse sands in different mortar mixes. Waste olive stone was pyrolyzed at 500 °C to produce the biochar. Water-cement ratio was kept constant at 0.5 for all mixes, whereas superplasticizer % increased with increasing BC dosage. Sand in the mixes was graded as S1 (2-4 mm), SII (1-2 mm) and SIII (smaller than 1 mm) and was mixed in 16%, 25% and 59% by weight of total

sand. Same size gradation was done for biochar as well and named BI, BII and BIII. In first three mixes, BI and BII replaced SI and SII sand at 25, 45 And 60% by volume of sand, and were designated as LWMB25, LWMB45 and LWMB60. The final mix had BI and BII as 25% replacement of SI and SII alongside 5% replacement of SIII with BIII. Compressive strengths of the mixes were tested in accordance to EN 1015-11-2019 on cube samples of the dimension 40*40*40 mm, at the ages of 7 and 28 days. It was found that 7 days compressive strengths of LWMB25, LWMB45 and LWMB60 reduced by 7, 9 and 11% w.r.t NWM, respectively. At 28 days, LWBM25 and LWBM60 showed strength reductions of 15% and 22% w.r.t NWM, respectively. LWMB25-5 mix had 7 and 28 days compressive strengths 16% and 25% lower than the NWM. This reduction was attributed to the porous nature of the olive stone biochar and the fact that biochar particle size was almost same as the particle size of the sand it replaced. These coarse biochar particles led to higher porosity and did not show very extensive filler effect. Thus it was seen that the biochar particle size also plays a very major role in the effect of biochar sand replacement on the mechanical properties of the mixes.

Zhang et al. (2024) studied the effect of replacing sand with four different types of biochars, i.e. palm shell biochar (1BR), apricot shell biochar (2BR), date shell biochar (3BR) and peach shell biochar (4BR) on UHPC Mixes. These biochars had very high iodine value of 600, which is a direct parameter representing the capacity of the biochars to adsorb high amount of pollutants including CO_2, by the virtue of high adsorption capacity, surface area and porosity. Water-cement ratio was kept constant at 0.24 throughout all the mixes. Only the mixes prepared with palm shell biochar (1BR) were subjected to comprehensive testing including the compressive strength testing. Mixes were prepared in accordance to the different dosage of the biochar used as replacement of the sand, which were 1%, 2%, 4%, 8%, 10%, 20%, 30% and 40%. Upon casting, samples underwent wet curing for 3 and 28 days. It was observed that 28 days compressive strengths of the mixes 1BR8, 2BR8, 3BR8 and 4BR8 were 5.25%, 10.70%, 6.99% and 11.14% lower than the control mix BR0. Upon studying the effect of incorporation of palm shell biochar at different dosages on the compressive strength, it was observed that at 1% biochar dosage(1BR1), both the 3 days and 28 days compressive strengths were higher than control group. This could be explained by the fact that the water present in the pores of biochar acting as nucleation sites, led to the formation of hydration products leading to denser matrix. 1BR2 had compressive strength comparable to the control mix. 1BR10 showed 3 days and 28 days compressive strengths 9.32% and 2.32% lower than the control, respectively. Similarly, 3 and 28 days compressive strengths of 1BR20, 1BR30 and 1BR40 were 29.62% and 23.59%, 44 and 39.89%, and 47.66% and 47.32% w.r.t the control mix, respectively. It was observed

that up to 1% dosage, biochar addition was proven to be feasible and marginally improved the compressive strength.

Sirico et al. (2021) had similar results in context to the effect of biochar as filler on splitting tensile strength. For this study, biochar was produced by the pyro-gasification process of wood waste biomass. In this study, aggregates were mixed in 2:1 ratio for fines (66.67%) and coarse aggregates (33.33%). Water-cement ratio was taken as 0.5:1. Four mixes were prepared namely BC-2.5, BC-5.0, BC-7.5 and BC-10.0 with biochar content being 2.5%, 5%, 7.5% and 10% respectively, in addition to the PC mix which was the control mix. For all the mixes, two types of curing were done, i.e. water curing and dry curing. D_{10} and D_{50} and D_{90} for biochar particles were found to be 11.4, 107 and 634 μm, respectively. Sand had maximum particle size of 4 mm with 81.8% passing 2 mm sieve, whereas the coarse aggregate had a maximum particle size of 10 mm with 83.9% passing through 8 mm sieve. It was observed that in dry curing regime, 28 days compressive strength increased by 25% and 17% for 2.5% and 5% biochar addition, w.r.t plain concrete, while the corresponding results at same replacement levels in the case of water curing are 5% and 3%, respectively. At replacement levels higher than 5%, compressive strength is affected negatively, more so for the water curing than for dry curing. 5% dosage was observed to be the overall optimal dosage. It was also observed that strength development, both short and long terms, was higher in the case of dry curing than the water curing. Internal curing effect of biochar was also observed as the strength development from 28 days to 365 days for the mix obtained with 5% biochar dosage, in dry curing case, was about 12%, whereas it was negligible for plain concrete mix. Similarly, for water curing, strength development from 28 to 365 days for 5% BC mix was 34% and 25% for plain concrete mix.

Tang and Qiu et. al (2024) lightweight concretes were developed using reactive magnesia cement, Sodium hexametaphosphate, NWAs (micro-silica sand, mean particle size 150 mu-m), very high amount of LWAs (BC or shale particles both finer than 1 mm, up to 61 vol% of concrete). Biochar was developed by the pyrolysis of peanut shells at 500 ◦C. For Mixes 0 to 160, RMC-to-biochar varied from 0 to 1.6. Water-cement ratio adopted was 0.79. Separately, S100 Mix was made with RMC, Silica sand, Oven dried Shales (instead of Biochar) and water as a reference (or control) to B100. Compressive strength decreased monotonically and significantly with the increasing content of biochar aggregate. 28 days compressive strength of biochar concrete decreased to 5.5 MPa for B60 to 11.9 MPa for B160, w.r.t 55.6 MPa for BC-free concrete. This trend was attributed to high porosity of BC and micro-defects introduced by it in the matrix. Additionally, unusually high dosage of biochar in the mixes is also a reason

for decreasing compressive strength. The explanation for this behaviour is that the quality of the binder and initial defects govern the strength, if biochar dosage is low. In such case, although BC results in higher porosity and more defects in the concrete matrix, it also enhances binder's pozzolanic reaction, i.e. pozzolanic effect. On the contrary, the strength and mechanical properties depend on the initial defects if BC dosage is high.

2.2.2 Flexural Strength

Praneeth et al. (2021) In this study, enhanced poultry litter was pyrolyzed to form biochar which was used as a filler material, as a replacement of sand, and its effect on the mixes was studied. Sand was replaced in the range of 10% to 40% of the total weight. Four mixes were prepared: B-0, B-10, B-20, and B-40, corresponding to 0, 10, 20, and 40% BC dosages, respectively. Water cement ratio used was 1:2.5 and water-binder ratio was 0.5. Average particles sizes in this study were Cement: 8.05 µm, sand: 311.75 µm and Biochar: 26 µm. It was observed that 28 days flexural strength increased up to 20% dosage of biochar as sand replacement and then decreased in the case of B-40. B-20 had the peak 28 days flexural strength at 6.3 MPa, a 26% improvement over control mix. This trend can be explained with the fact that the carbon in biochar occupied the pores between sand particles when biochar was mixed with sand in the composite, this caused reduction in toughness. When these biochar particles were met with the path of crack propagation, it caused many finer cracks passing through weaker areas. This deviation of the crack propagation accounted for requirement of more fracture energy to break the biochar as would be needed for cement or sand.

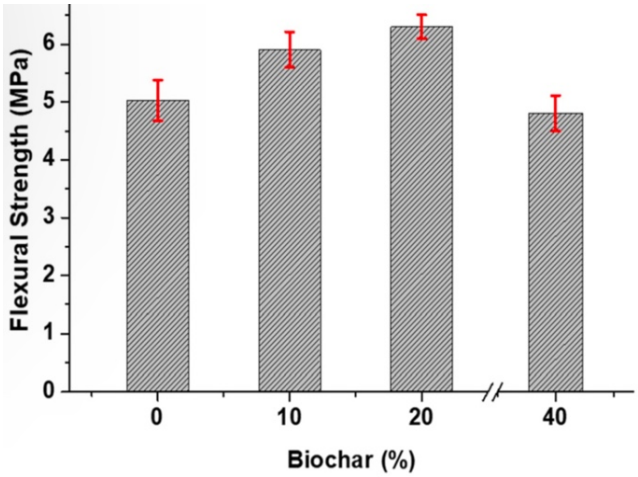

Figure 2.15 Flexural strength of different mixes (Praneeth et al. 2021)

Zhang et al. studied the effect of replacing sand with four different types of biochars, i.e. palm shell biochar (1BR), apricot shell biochar (2BR), date shell biochar (3BR) and peach shell biochar (4BR) on UHPC Mixes. These biochars had very high iodine value of 600, which is a direct parameter representing the capacity of the biochars to adsorb high amount of pollutants including CO_2, by the virtue of high adsorption capacity, surface area and porosity. Water-cement ratio was kept constant at 0.24 throughout all the mixes. Only the mixes prepared with palm shell biochar (1BR) were subjected to comprehensive testing including the flexural strength testing. Mixes were prepared in accordance to the different dosage of the biochar used as replacement of the sand, which were 1%, 2%, 4%, 8%, 10%, 20%, 30% and 40%. Upon casting, samples underwent wet curing for 3 and 28 days. Flexural strength was investigated and it was found that flexural strength decreased considerably when biochar dosage was over 10%. Beyond that, flexural strength had very sharp decline at 30% and 40% dosages. This was primarily due to high biochar dosage causing weaker interfaces at Interfacial transition zones causing irregularities in the internal structure of the matrix.

Sirico et al. (2021) studied the effect of biochar derived from the pyro-gasification of forest wood waste, used as filler in cementitious mixes. For this study, biochar was produced by the pyro-gasification process of wood waste biomass. D_{10}, D_{50} and D_{90} for biochar particles were found to be 11.4, 107 and 634 μm, respectively. Sand used had a maximum particle size of 4 mm, with 81.8% particles passing 2 mm sieve, whereas coarse aggregate used was a siliceous stone having maximum particle size of 10 mm, with 83.9% passing 8 mm sieve. Reference mix for this study had oven dried aggregates mixed in 2:1 ratio for fines (66.67%) and coarse aggregates (33.33%). Water-cement ratio was taken as 0.5:1. Four more mixes were prepared namely BC-2.5, BC-5.0, BC-7.5 and BC-10.0 with biochar being added to the PC Mix at 2.5%, 5%, 7.5% and 10% by weight of cement, respectively. For all the mixes, two types of curing were done, i.e. water curing and dry curing. Flexural strength testing was done under three-point loading in accordance to the standard guidelines laid down in JCI-S-001. For both dry and water curing, flexural strength for biochar mixes improved, w.r.t the plain concrete mix. Peak values of flexural strength in the case of dry curing was for the mix with 5% biochar dosage and was 29% higher than plain concrete, whereas in the case of water curing, maximum enhancement was of 27% w.r.t the plain mix, for the mix with 2.5% biochar dosage. Plain mix and biochar mixes showed no major differences in terms of the strength development between 28 and 365 days.

2.2.3 Splitting Tensile Strength

Sirico et al. (2021) had similar results in context to the effect of biochar as filler on splitting tensile strength. For this study, biochar was produced by the pyro-gasification process of wood waste biomass. In this study, aggregates were mixed in 2:1 ratio for fines (66.67%) and coarse aggregates (33.33%). Water-cement ratio was taken as 0.5:1. Four mixes were prepared namely BC-2.5, BC-5.0, BC-7.5 and BC-10.0 with biochar content being 2.5%, 5%, 7.5% and 10% respectively, in addition to the PC mix which was the control mix. For all the mixes, two types of curing were done, i.e. water curing and dry curing. D_{10} and D_{50} and D_{90} for biochar particles were found to be 11.4, 107 and 634 μm, respectively. Sand had maximum particle size of 4 mm with 81.8% passing 2 mm sieve, whereas the coarse aggregate had a maximum particle size of 10 mm with 83.9% passing through 8 mm sieve. Splitting tests showed that the splitting tensile strength increased w.r.t the control mix up to 5% biochar dosage, both in the cases of dry and water curing. At dosages higher than 5%, splitting tensile strength decreased in the case of water curing, whereas it had marginally positive effects in the case of dry curing. Overall, it was noticed that tensile behaviour of the mixes was considerably less affected with biochar addition as compared to the flexural and compressive strengths.

2.2.4 Shrinkage

Sirico et al. (2021) had similar results in context to the effect of biochar as filler on splitting tensile strength. For this study, biochar was produced by the pyro-gasification process of wood waste biomass. In this study, aggregates were mixed in 2:1 ratio for fines (66.67%) and coarse aggregates (33.33%). Water-cement ratio was taken as 0.5:1. Four mixes were prepared namely BC-2.5, BC-5.0, BC-7.5 and BC-10.0 with biochar content being 2.5%, 5%, 7.5% and 10% respectively, in addition to the PC mix which was the control mix. For all the mixes, two types of curing were done, i.e. water curing and dry curing. D_{10} and D_{50} and D_{90} for biochar particles were found to be 11.4, 107 and 634 μm, respectively. Sand had maximum particle size of 4 mm with 81.8% passing 2 mm sieve, whereas the coarse aggregate had a maximum particle size of 10 mm with 83.9% passing through 8 mm sieve. With the help of strain measurements, it was found that up to 60 days after casting, shrinkage in the reference mix and the mix with 5% biochar dosage were almost comparable.

Zhang et al. studied the effect of replacing sand with four different types of biochars, i.e. palm shell biochar (1BR), apricot shell biochar (2BR), date shell biochar (3BR) and peach shell biochar (4BR) on UHPC Mixes. These biochars had very high iodine value of 600, which is a direct parameter representing the capacity of the biochars to adsorb high amount of pollutants

including CO_2, by the virtue of high adsorption capacity, surface area and porosity. Water-cement ratio was kept constant at 0.24 throughout all the mixes. Only the mixes prepared with palm shell biochar (1BR) were subjected to comprehensive testing including the flexural strength testing. Mixes were prepared in accordance to the different dosage of the biochar used as replacement of the sand, which were 1%, 2%, 4%, 8%, 10%, 20%, 30% and 40%. Upon casting, samples underwent wet curing for 3 and 28 days. It was observed that in initial stages, addition of palm shell biochar resulted in increase in drying shrinkage, which later reduced beyond 10 days age. Drying shrinkage reduced at replacement levels under 8% and increased considerably at 30 and 40% replacement levels. It could be summarized that autogenous shrinkage decreased with increasing dosage of biochar. Type of biochar had a major effect on drying shrinkage. At 8% replacement level, mix with date shell biochar had lower autogenous shrinkage strain than the mix with apricot shell biochar.

2.2.5 Water Absorption

Praneeth et al. (2021) In this study, enhanced poultry litter was pyrolyzed to form biochar which was used as a filler material, as a replacement of sand, and its effect on the mixes was studied. Sand was replaced in the range of 10% to 40% of the total weight. Four mixes were prepared: B-0, B-10, B-20 and B-40 corresponding to 0, 10,20 and 40% BC dosages, respectively. Water cement ratio used was 1:2.5 and water-binder ratio was 0.5. Average particles sizes in this study were Cement: 8.05 µm, sand: 311.75 µm and Biochar: 26 µm. Overall, it was observed that water absorption and voids increased with increasing biochar content. B-40 had a water absorption of 21.3%. This increasing trend of water absorption is primarily because of the high water retention capacity of biochar due to high surface area. Size of biochar particles play a significant role in the water absorption trends.

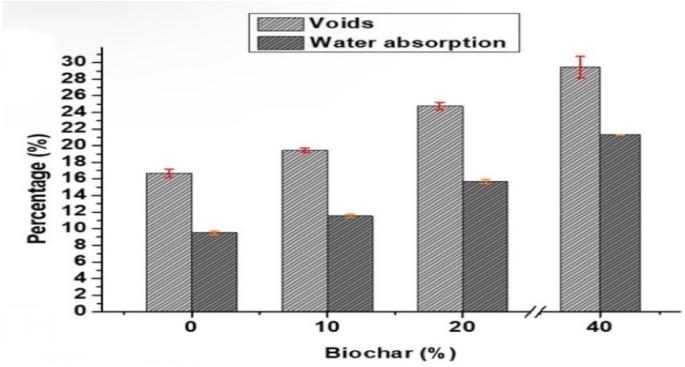

Figure 2.16 Water absorption for different mixes (Praneeth et al. 2021)

Maljaee et al. (2022) studied the effect of replacing olive stone waste biochar as a replacement of coarse sands in different mortar mixes. Waste olive stone was pyrolyzed at 500 °C to produce the biochar. Water-cement ratio was kept constant at 0.5 for all mixes, whereas superplasticizer% increased with increasing BC dosage. Sand in the mixes was graded as S1 (2-4 mm), SII (1-2 mm) and SIII (smaller than 1 mm) and was mixed in 16%, 25% and 59% by weight of total sand. Same size gradation was done for biochar as well and named BI, BII and BIII. In first three mixes, BI and BII replaced SI and SII sand at 25, 45 And 60% by volume of sand, and were designated as LWMB25, LWMB45 and LWMB60. The final mix had BI and BII as 25% replacement of SI and SII alongside 5% replacement of SIII with BIII. It was observed that water absorption of the mixes increased with increasing biochar dosage. LWMB25, LWMB45 and LWMB60 had 25%, 42% and 60% higher water absorption than the reference mix. This was caused to high porosity of the biochar as compared to sand, which meant higher pore area available for water to be absorbed. Additionally, particle morphology also played an important role as Olive stone biochar particles are spherical in nature.

2.2.6 CO_2 Sequestration and emissions

Praneeth et al. (2021) In this study, enhanced poultry litter was pyrolyzed to form biochar which was used as a filler material, as a replacement of sand, and its effect on the mixes was studied. Sand was replaced in the range of 10% to 40% of the total weight. Four mixes were prepared: B-0, B-10, B-20 and B-40 corresponding to 0, 10,20 and 40% BC dosages, respectively. Water cement ratio used was 1:2.5 and water-binder ratio was 0.5. Average particles sizes in this study were Cement: 8.05 μm, sand: 311.75 μm and Biochar: 26 μm. It was found that net CO_2 generation from the production of poultry litter biochar was -0.49 kg of CO_2 equivalents per kg of biochar, whereas this figure for cement and sand were approximately 1.002 kg CO_2 equivalents/ kg of cement and 9.87 $\times 10^{-3}$, respectively. Since biochar partially replaced sand, net emissions of the mixes ultimately lowered. Upon calculations, it was established that net CO_2 emissions decreased from 508 kg for B-0 to 405 kg for B-40.

Zhang et al. studied the effect of replacing sand with four different types of biochars, i.e. palm shell biochar (1BR), apricot shell biochar (2BR), date shell biochar (3BR) and peach shell biochar (4BR) on UHPC Mixes. These biochars had very high iodine value of 600, which is a direct parameter representing the capacity of the biochars to adsorb high amount of pollutants including CO_2, by the virtue of high adsorption capacity, surface area and porosity. Water-

cement ratio was kept constant at 0.24 throughout all the mixes. Only the mixes prepared with palm shell biochar (1BR) were subjected to comprehensive testing including the flexural strength testing. Mixes were prepared in accordance to the different dosage of the biochar used as replacement of the sand, which were 1%, 2%, 4%, 8%, 10%, 20%, 30% and 40%. Upon casting, samples underwent wet curing for 3 and 28 days. It was observed that net CO_2 emissions went down from 4.4415×10^{-3} kg for BR0 to 2.6649×10^{-3} kg for BR40, meaning a drop of over 40%.

2.3 Synthetic Biochar aggregate or other Light weight aggregates (LWAs) replacement.

2.3.1 Compressive Strength

Wyrzykowski et al (2024) studied the unconventional method of incorporating biochar in cementitious mixes, i.e. cold bonded light weight aggregates (LWAs). In this study, landscape and gardening waste base biochar, made by pyrolysis of biomass at 680 ◦C was used to make Cold-bonded light weight aggregates. Thick slurry mix of cement, dried biochar and water in the ratio 1:2:2.4 were mixed in rotary mixer and pelletized, resulting in disintegration of larger pieces of the slurry. This “green” mix in the form of pellets were stored at high humidity (over 90% RH) and room temperature until cement hardening to obtain C-LWA. C-LWA size used in this study were 8-20 mm, with 40% fraction smaller than 8 mm and equal fraction larger than 20 mm. C-LWAs were added to the mixes in three forms: i) C-LWA saturated-0.53: pre-saturated with extra water for 24 hours (i.e. the water absorbed by C-LWAs, which is in addition to the mixing water), w/c ratio=0.53 ii) C-LWA-saturated-0.40: pre-saturated with mixing water for 24 hours (i.e. without any extra water), w/c ratio= 0.40 iii) C-LWA dry-0.40: unsaturated C-LWAs, (i.e. without any extra water). It was determined that compressive strength of the concretes decreased by 6%, 9% and 23% when mixed with C-LWA saturated-0.40, C-LWA dry-0.40 and C-LWA saturated-0.53 as NWA replacement, respectively.

Rajesh Kumar et al. (2023) reported the effect of using Lightweight expanded clay aggregate, fly ash and marble slurry in lightweight aggregate concretes on its mechanical properties such as compressive strength. Mix design in this study was done on the basis of optimization of different components of the concrete mixes. In case 1, aggregates and water-cement ratios were

optimized and mixes prepared were MA-1, MA-2, MA-3, MA-4, MA-5 and MA-6. corresponding to different proportions of three different LECA sizes: 0-2 mm, 2-8 mm and 8-15 mm, while keeping cement and sand content same. MA-3 was found to be the optimal mix in this case. In case 2, superplasticizer % and slump were optimized and mixes prepared were MS-1, MS-2, MS-3, MS-4, MS-5 and MS-6 corresponding to different water-cement ratio and Superplasticizer%, keeping LECA% Constant corresponding to MA-3 from case 1 optimization. In case 2, MS-3 was found to be the optimal mix. In case 3, cement content was optimised. Mixes prepared were MC-1, MC-2, MC-3, MC-4 and MC-5 were made corresponding to different cement content while keeping Superplasticizer, water-cement ratio, sand content and LECA% constant. MC-5 mix was found to be optimal. In case 4, fly ash and marble slurry content was optimised and the mixes prepared were M-1, M-2, M-3 and M-4 corresponding to different fly ash% and Marble slurry%, while keeping cement, sand, water-cement ratio, Superplasticizer % and LECA% constant in accordance to their optimal values from first three cases of optimization, i.e. MA-3 for LECA%, MS-3 for water-cement ratio and Superplasticizer%; and MC-5 for cement content.

2.3.2 CO_2 Sequestration

Wyrzykowski et al (2024) studied the unconventional method of incorporating biochar in cementitious mixes, i.e. cold-bonded lightweight aggregates (LWAs). In this study, landscape and gardening waste base biochar, made by pyrolysis of biomass at 680 ◦C was used to make Cold-bonded light weight aggregates. A thick slurry mix of cement, dried biochar and water in the ratio 1:2:2.4 was mixed in a rotary mixer and pelletized, resulting in the disintegration of larger pieces of the slurry. This “green” mix in the form of pellets were stored at high humidity (over 90% RH) and room temperature until cement hardening to obtain C-LWA. C-LWA size used in this study were 8-20 mm, with 40% fraction smaller than 8 mm and equal fraction larger than 20 mm. C-LWAs were added to the mixes in three forms: i) C-LWA saturated-0.53: pre-saturated with extra water for 24 hours (i.e. the water absorbed by C-LWAs, which is in addition to the mixing water), w/c ratio=0.53 ii) C-LWA-saturated-0.40: pre-saturated with mixing water for 24 hours (i.e. without any extra water), w/c ratio= 0.40 iii) C-LWA dry-0.40: unsaturated C-LWAs, (i.e. without any extra water). Gross emissions from reference concrete were estimated at 207 kg CO_2/m^3 of concrete. These high emissions can be cut down using biochar aggregates, and even further reduced using cold bonded aggregates due to their high

C-sink potential. Consequently, C-LWA concrete mixes studied in this study showed net-zero emissions due to high dosage of C-LWA in the mixes. Emissions from C-LWA were -1.05 CO_2/kg of C-LWA when in cured state. Hence, this is a significant improvement over conventionally hardened LWAs using the sintering process, which usually occurs at around 900-1200 ◦C, as sintered LWAs account for an additional 10-13 kg CO_2/m^3.

Zou et al. (2024) investigated the properties of the concrete incorporating artificially manufactured core-shell aggregates. Biochar used in this study was prepared by the pyrolysis of waste corncob at 500 ℃ for a residence time of 2 hours. Produced biochar was sieved to 2.36-4.75 mm for the production of the aggregates. Ground granulated blast furnace slag (GGBS) was used to replace the cement in 0%, 20%, 40%, 60%, 80% and 90% dosages for the preparation of the shell of CSA, purpose of this GGBS replacement being the reduction of emissions. Water-binder ratio adopted for manufacturing Biochar-CSA was 0.21. Ratio of masses for the production of shell and core was 8 (shell-to-core). Biochar-CSA produced artificially was employed as the replacement of normal weight natural aggregates. For the mix MC0, only natural aggregates and no Biochar-CSA were used. Water-binder ratio adopted was 0.3. MC30, MC60 and MC90 mixes were made with 30%, 60%. and 90% natural aggregates being replaced with Biochar-CSA, respectively. Sizes of the natural fine aggregate, natural coarse aggregate and Biochar-CSA were in the range of 0-4.75 mm, 4.75-10 mm and 0-10 mm respectively. It was calculated that production of 1 ton of Biochar-CSA with 100% OPC used in shell, released 361 kg of CO_2 in total (including materials, transport and production). Materials were responsible for almost 93% emissions from the Biochar-CSA. This highlights the importance of cold-bonding method of production of the Biochar based LWAs. It was also observed that when GGBS was used to replace cement in the production of biochar, CO_2 decreased from 361 kg to -123 kg for 90% GGBS replacement. Since peak mechanical properties of the LWAC were observed when MG80 Biochar-CSA was used, it was used for the preparation of the mixes and extensive testing.

CHAPTER 3

MATERIALS AND METHODOLOGY

3.1 Introduction

This chapter outlines the materials used and the experimental methodology adopted to investigate the influence of rice straw–derived biochar as a partial replacement for Ordinary Portland Cement in structural concrete. The study involved systematic preparation, casting, curing, and testing of concrete specimens designed at predefined replacement levels to evaluate changes in fresh, mechanical, and durability properties. The methodology includes detailed characterization of biochar, mix proportioning, sample preparation procedures, test protocols, and instrumentation used. By presenting a clear and reproducible experimental framework, this chapter ensures scientific rigor and facilitates accurate interpretation of results, while providing essential context for comparing the performance of biochar-modified concrete with conventional concrete mixtures.

3.2 Materials used

3.2.1 Cement

In this investigation, JK Super Ordinary Portland cement of grade 43 (OPC 43) was used, which complies with ASTM C150M (ASTM 2016) and BIS 8112:2013 (BIS 2013). The consistency and setting time of the cement were determined using the BIS 4031-1989 (BIS 1989) standard.

3.2.1.1 Setting time

The BIS: 4031 (Part 5)-1988 provisions were applied to ascertain the cement's setting time. To create the cement paste, 0.85 times as much water was added as was required to achieve the required cement consistency. A trowel was used to level the entire mixture after it had been put into the mould. Under the mould, the rod bearing needle was stored. The top surface of the mould was penetrated by the needle when it was lowered. The process was repeated until the needle could only pierce the mould 5.0 mm from the bottom. The first setting time is calculated

from the moment water is poured to the cement until the needle, inserted from the bottom, cannot penetrate more than 5.0 mm.

The final setting time is calculated from the time water is added to the cement until the time an impression is formed on the surface of the test sample. The final setting time is measured with a needle with an annular collar. The cement is fully set when an impression is formed on the specimen's surface after a gentle contact by the needle on the surface.

3.2.1.2 Consistency

Cement consistency refers to the minimum quantity of water incorporated into cement to produce a uniform paste with appropriate viscosity and strength for diverse structural applications. The cement's consistency was assessed according to the BIS: 4031 technique (BIS 1989). A 500g cement paste was initially made and placed in the Vicat mould. The upper surface of the mould was levelled, and any unwanted air was eliminated by shaking it. The rod with a plunger of the Vicat equipment was employed to secure the mould. The plunger was lowered to contact the upper surface of the mould. Experimental mixtures of pastes with varying water quantities were utilised to ascertain the precise volume of water required to achieve the intended consistency. Results of various properties of JK Super Ordinary Portland Cement Grade 43 used in this study are tabulated as follows:

Table 3.1 Properties of OPC 43

Tests	Results	Standard results as per IS:8112-2013
Specific Gravity	3.21	-
Normal Consistency (%)	28	-
Fineness (m^2/kg)	291	≥ 225
Initial setting time (min)	45	≥30
Final setting time (min)	270	≤600

3.2.2 Coarse aggregate

Aggregates above 4.75 mm in size are classified as coarse aggregates. They regulate the strength characteristics of concrete. Coarse aggregates with a specific gravity of 2.78 were utilised, and the water absorption of the aggregates was 0.73 %. The 10mm coarse aggregates were obtained from quarries in Pathankot.

Table 3.2 Properties of Coarse aggregate

S. No.	Property	Results
1	Fineness modulus	6.003
2	Specific gravity	2.78
3	Water absorption	0.73%

3.2.3 Fine aggregate

These are aggregates having a diameter of 4.75 mm or smaller. Particles pass from a 4.7 mm sieve and are retained by a 75 micron sieve. These are critical for regulating fundamental cement characteristics like workability. The experimental program utilised fine aggregates locally sourced river sand as fine aggregate, which was in accordance with the stipulations of BIS: 383-1970 (BIS 1970), which is comparable to ASTM C33/C33M (ASTM 2018). The initial source of fine aggregates was taken from Pathankot, Punjab, India. The gathered fine aggregates exhibited a specific gravity of 2.6, a fineness modulus of 2.32, and a water absorption rate of 1.49%.

Table 3.3 Properties of Fine aggregate

S. No.	Property	Results
1	Zone of Sand	Zone II
2	Fineness modulus	2.327
3	Specific gravity	2.6
4	Water absorption	1.49%

Sieve analysis of the sand was conducted as per the guidelines of IS:2386 (Part 1)-1963. A sample of the sand was taken and was heated in the oven for a period of 24 hours at a temperature of approximately 100° C in order to remove all its moisture. Sieve analysis is then conducted on 1000 grams sample of this dried sand in the sieve shaker in order to obtain particle size gradation.

Figure 3.1 Mechanical sieve shaker used for sieve analysis of fine aggregate

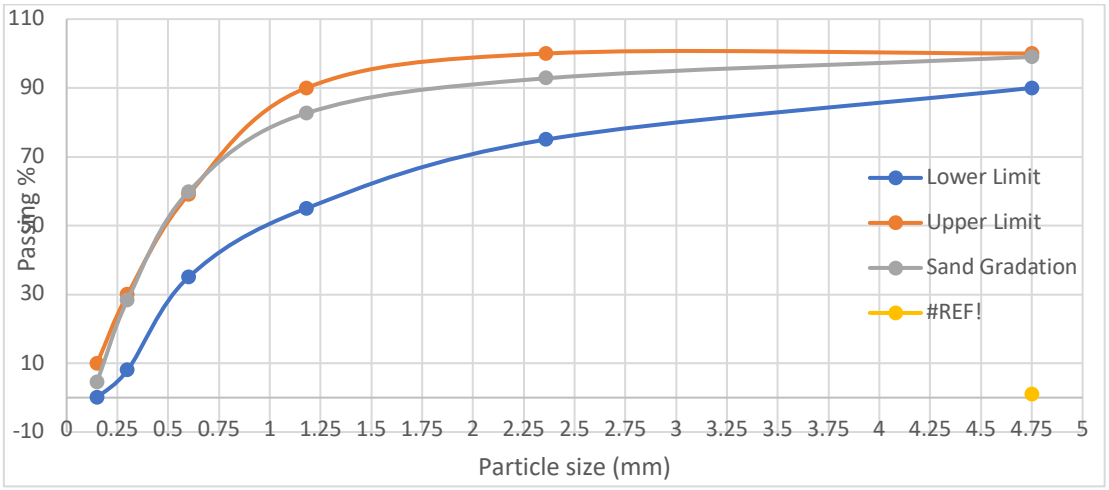

Figure 3.2 Particle size gradation curve of fine aggregate

3.2.4 Biochar

Biochar was produced using rice straw waste as the source biomass. Biomass was procured from a farm from a nearby village in Patiala district, after the paddy harvesting season. The straws were washed in water, and the water was drained to remove dirt, small stones, leaves, and other debris and unwanted materials. The biomass was then sun-dried and subsequently dried in an oven for 24 hours at 100 °C to remove all surface moisture and prepare the biomass for pyrolysis. Upon drying, the biomass was placed in clay crucibles, covered with a clay lid, and then placed in a programmable muffle furnace for pyrolysis. The samples underwent pyrolysis at 550°C for 2 hours at a rate of 10°C/min in the presence of limited oxygen. The furnace was allowed to cool down upon pyrolysis and then produced biochar is then cooled

down to the room temperature and stored in air-tight containers. Before mixing and other tests, biochar was ground so as to ensure a particle size distribution comparable to that of the Ordinary Portland Cement. Biochar's specific gravity was calculated to be 1.4. Upon taking the weights of the biomass before pyrolysis and produced biochar, it was calculated that approximate yield of the biomass was approximately 37%, i.e. pyrolysis of 1 kg cleaned and dried rice straw waste gave approximately 370 grams of biochar.

Ground biochar had a median size (D_{50}) of 1.23 µm, as reported in *Rashid et al (2026)*.Same particle size is valid for this study as the biochar was processed for this study and *Rashid et al (2026)* together at the same time. D_{90} of the ground biochar was 2.21 µm. In contrast, D_{50} and D_{90} for Ordinary Portland cement used in this study were 9.42 µm and 14.9 µm. Thus it is evident biochar, being much smaller than cement particles, exhibited filler effect, occupying voids in the concrete matrix.

Figure 3.3 Different stages of biochar production

Different stages of biochar production are shown in Figure 19. Where (a) shows the rice stubble waste as was used as raw feedstock for the production of biochar, (b) shows programmable

muffle furnace (c) shows biochar as produced as the pyrolysis product, and (d) ground biochar as used in concrete in this study.

3.2.5 Water

Normal potable water with a pH ranging between 6.5 and 8.5, was used at ambient temperature for mixing all ingredients for the production of structural concrete.

3.2.6 Admixture

MasterGlenium 51, a modified polycarboxylic ether (PCE) polymer based high-range water reducing admixture (or Superplasticizer) was used in all the mixes in uniform quantity. As per the specifications provided by its manufacturer, MASTER® BUILDERS SOLUTIONS, this admixture is compliant with EN 934-2: T3.1 and T3.2; and its specific gravity is approximately 1.10 g/cm^3. Its pH value was reported at 6.75.

3.3 Mix design

A control mix was first made as the reference mix with no replacement of the Ordinary Portland Cement with Biochar, i.e. 0% biochar. Subsequent mixes had increasingly higher quantity of biochar introduced in the mix as the partial replacement of the OPC at 2.5%, 5%, 7.5% and 10% by the weight of the OPC, and the mixes were designated as M-1, M-2, M-3 and M-4 respectively. Dry aggregates were mixed first and the dry mix of the cement and biochar was added to the dry aggregates mix in a pan mixer and the entire dry mix was mixed in the pan mixer while half the prescribed quantity of the water being added to the mix while the mixer was rotated for about 2 minutes. Following which the remaining water mixed with the Super-plasticizer was added to the mixed and the mixer was rotated for about 4 minutes.
A constant water-binder ratio of 0.45 was maintained throughout all the mixes in order to observe the effect of adding biochar and its high water-absorbing capacity on the properties of concrete.

Table 3.4 Final mix design

S. No.	Mix	Cement	Fine aggregate	Biochar	Coarse aggregate	Water	Water-binder ratio	Admixture* (HR-WRA)
		kg/m^3	kg/m^3	kg/m^3	kg/m^3	kg/m^3		kg/m^3
1	M-0	406.2	662	0	1201	182.79	0.45	4.062
2	M-1	396.05	662	10.155	1201	182.79	0.45	4.062
3	M-2	385.89	662	20.31	1201	182.79	0.45	4.062
4	M-3	375.74	662	30.465	1201	182.79	0.45	4.062
5	M-4	365.58	662	40.62	1201	182.79	0.45	4.062

*Superplasticizer used at the rate of 1% of the weight of total binder ; i.e. Cement and Biochar, in all the mixes

3.4 Preparation, casting and curing of concrete specimens

Prior to casting, the physical properties of all constituent materials were evaluated and found satisfactory, after which the aggregates were soaked and surface-dried to ensure proper moisture condition before mixing. The dried fine and coarse aggregates were first blended in the pan mixer, followed by combining biochar with Ordinary Portland Cement and mixing thoroughly until a uniformly darker shade of cementitious material was achieved, with colour intensity increasing proportional to biochar content. Water and superplasticizer were premixed carefully to minimize loss during handling. The moulds were properly cleaned, tightened, and lubricated before casting commenced. Subsequently, the dry aggregate blend and the cement–biochar mixture were added to the mixer, followed by gradual addition of half the water, and finally the remaining water containing superplasticizer; mixing was continued for approximately 5 minutes to achieve uniform consistency. Concrete specimens were prepared using 100×100×100 mm cube moulds, 100×200 mm cylinder moulds, and 100×100×500 mm prism moulds. After casting, samples were kept undisturbed at ambient conditions for 24 hours to allow setting, after which they were demoulded, weighed for density determination, and placed in water for curing at room temperature for 7 and 28 days. Upon completion of the curing period, the hardened samples were retrieved and subjected to various mechanical and durability tests as part of the experimental analysis.

Figure 20 shows the casting process of concrete specimens where (a) is the fresh (green) concrete casted in the moulds, (b) hardened concrete specimens before de-moulding and (c) is the demoulded concrete specimens after curing and ready to be tested.

Figure 3.4 Casting process

3.5 Fresh state properties

3.5.1 Workability and Flow

Workability of the fresh concrete was evaluated through the slump test to determine its flow characteristics, as prescribed in IS 1199 (1959). The fresh green concrete was extracted directly from the mixer and placed into a properly lubricated slump cone in four successive layers, with each layer compacted using 25 evenly distributed blows from a tamping rod to ensure uniform consolidation. After the final layer was filled, the top surface was levelled smoothly using a trowel. The slump cone was then carefully lifted vertically, allowing the concrete to deform freely under its own weight. The resulting slump was measured as the vertical distance between the top of the mould and the displaced top surface of the slumped concrete, providing quantitative indication of the mix's workability and flowability.

Figure 3.5 Slump cone test

3.6 Non-destructive testing of hardened and cured concrete

3.6.1 Rebound hammer test

The rebound hammer test was performed using an N-type Schmidt rebound hammer (PROCEQ), in accordance with IS 13311 (Part 2) and IS 516 (Part 5/Section 4):2020, to assess the relative surface hardness and indicative strength of the concrete through measured rebound numbers. Cube specimens of 100 mm were tested after 28 days of curing, ensuring that the test surfaces were dry and clean prior to measurement. The hammer was positioned perpendicular to the specimen surface, and ten readings were taken at distinct, non-overlapping locations to avoid repetition at the same point of impact. Additionally, the cube samples were firmly held

in position between two plates of the UTM to ensure stability during impact, thereby enabling accurate and consistent rebound index measurements.

Figure 3.6 Rebound hammer test

3.6.2 Ultrasonic pulse velocity test

The ultrasonic pulse velocity (UPV) test was conducted in compliance with IS 13311 (Part 1) and IS 516 (Part 5/Section 1):2018 to assess the internal quality and uniformity of the concrete specimens. The apparatus used was a PROCEQ UPV device equipped with a 54 kHz transducer frequency. The equipment consists of two battery-powered probes one functioning as the transmitter that generates and introduces ultrasonic waves into the specimen, and the other serving as the receiver to detect the transmitted pulse either on the opposite surface (direct transmission) or on an adjacent side (semi-direct transmission). The measured travel time of the ultrasonic wave passing through the concrete was recorded, and this value was subsequently used to compute the pulse velocity, providing insight into the density, homogeneity, and presence of internal discontinuities within the concrete.

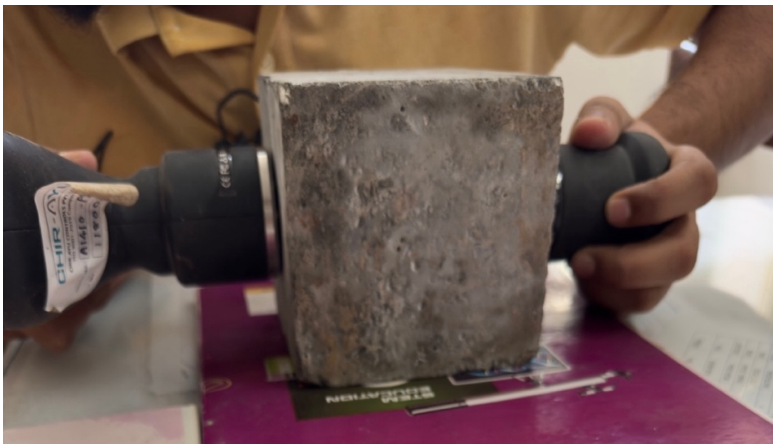

Figure 3.7 Ultrasonic pulse velocity test

3.7 Mechanical and strength properties

3.7.1 Compressive strength

The compressive strength of the concrete specimens was evaluated in accordance with IS 516 (Part 1/Sec 1):2021. Cube samples of 100 × 100 × 100 mm dimensions were tested after 28 days of curing. Prior to testing, the specimen surfaces were wiped to remove excess moisture. The cubes were placed centrally between the platens of the compression testing machine, ensuring uniform load distribution. Load was applied at a constant rate of stress until specimen failure, and the maximum load at failure was recorded. Compressive strength was computed by dividing the failure load by the loaded area, providing a direct measure of the concrete's ability to withstand axial compressive stresses.

Figure 3.8 (a) Compressive strength test (b) Compression failure pattern

3.7.2 Splitting tensile strength

The splitting tensile strength test was performed on cylindrical specimens of 100 mm diameter and 200 mm height, following IS 5816:1999. The cylinders were positioned horizontally between the curved jaws of the compression testing machine so that the applied load acted along a vertical diametral plane. As load increased, tensile stresses were induced across the vertical diameter, leading to longitudinal splitting of the specimen. The maximum load at failure was recorded, and the splitting tensile strength was calculated based on standard formula as given in equation 3.1, thereby assessing the material's tensile resistance.

$$f'st=2P/\pi l d. \quad (3.1)$$

where,

P= Peak load

l= Length of specimen

d= Diameter of the specimen

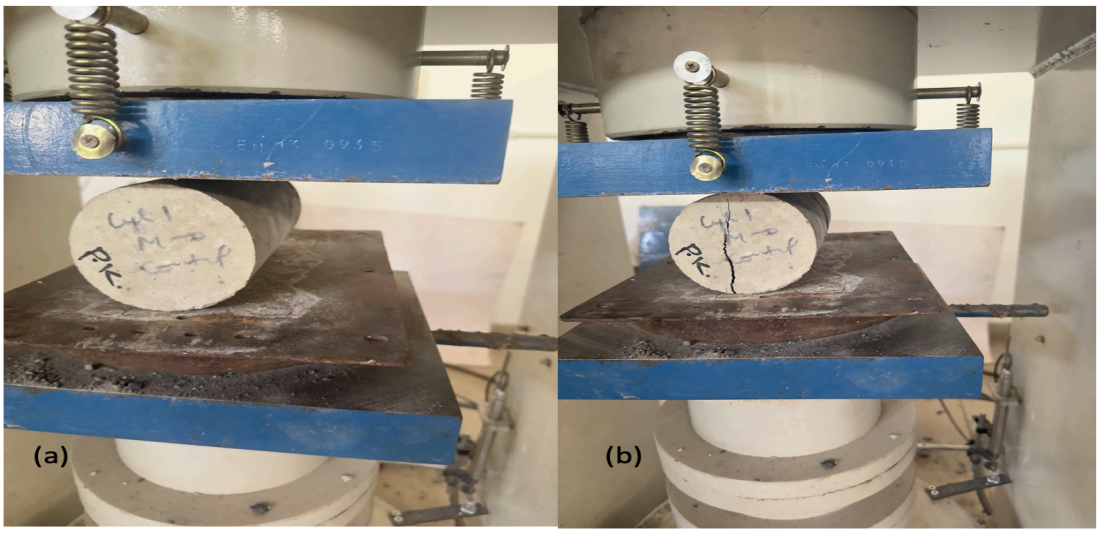

Figure 3.9 (a) Splitting tensile test set-up (b) Split tensile failure pattern

3.7.3 Flexural strength

Evaluation of flexural strength was carried out using prismatic beam specimens of 100 × 100 × 500 mm, tested as per IS 516 (Part 2/Sec 1):2020. The beams were subjected to the two-point loading method (third-point loading), ensuring a constant bending moment across the middle third of the span. Load was applied gradually until fracture occurred, and the maximum load was noted. Flexural strength (modulus of rupture) was determined as per the equation 3.2, to quantify the concrete's ability to resist bending and tensile stresses encountered in structural applications such as slabs and pavements.

$$R = Pl/bd^2 \quad (3.2)$$

Where,

R= Flexural strength (MPa)

P= Peak load (N)

l= Loading span (mm)

b= Width of the sample (mm)

d= Depth of the sample (mm)

Figure 3.10 Flexural strength test set-up

3.8 Durability properties

3.8.1 Rapid chloride permeability test

Resistance to chloride ion penetration was assessed using the Rapid Chloride Permeability Test (RCPT) in accordance with ASTM C1202. Disc-shaped specimens were sliced from the cured cylinders and vacuum-saturated prior to testing. Each specimen was placed between two fluid cells—one containing sodium chloride solution and the other containing sodium hydroxide—across which a constant electrical potential was applied for six hours. The total charge passed, measured in Coulombs, was recorded as an indicator of ionic permeability. Lower charge values indicated superior resistance to chloride ingress and enhanced durability against steel reinforcement corrosion.

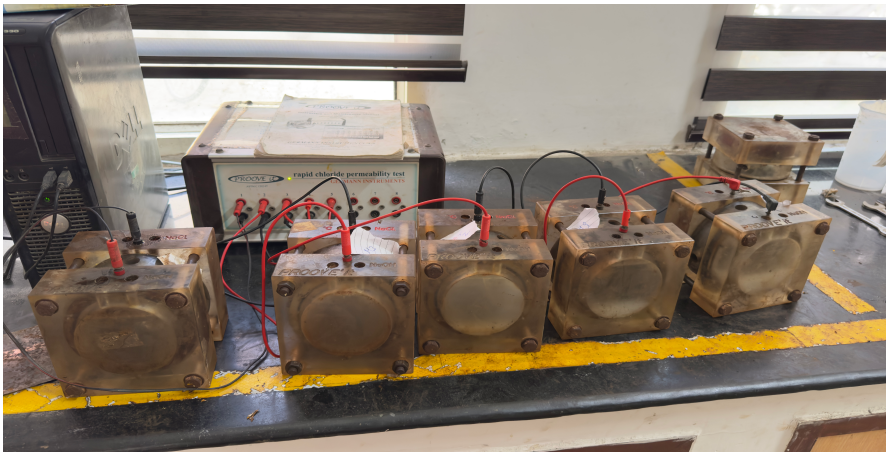

Figure 3.11 Rapid chloride permeability test set-up

Table 3.5 Chloride ion penetration levels based on charge passed (ASTM C 1202-10)

Charge passed (coulombs)	Chloride ion permeability
>4000	High
4000-2000	Moderate
2000-1000	Low
1000-100	Very low
<100	Negligible

3.8.2 Water Absorption

The water absorption characteristics of the hardened concrete were examined in accordance with IS 2185 and related guidelines. Specimens were oven-dried at 105°C until constant mass was achieved and were subsequently allowed to cool to ambient temperature. The dry mass was recorded before the samples were submerged in water for a specified absorption period. After immersion, the saturated mass was measured. Water absorption was calculated as the percentage increase in mass as per equation 3.3, providing insight into the permeability and pore structure of the concrete matrix influenced by biochar incorporation.

Water absorption, % is reported using following formula given in Equation 3.3

$$\text{Absorption, \%} = [(B-A)/A] * 100 \quad (3.3)$$

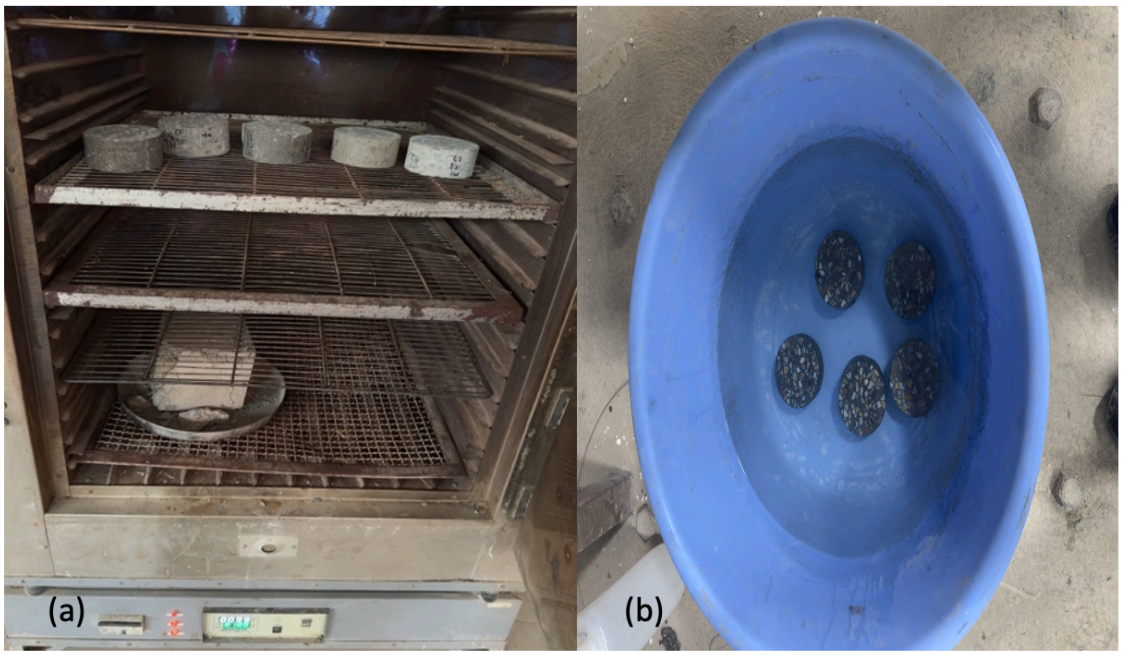

Figure 3.12 (a) Water absorption test samples oven dried to get weight "A" (b) Water absorption samples soaked in water to get weight "B"

3.9 Microstructural analysis and characterization

3.9.1 X-Ray diffraction analysis

X-ray diffraction (XRD) analysis was performed on powdered samples obtained from the core regions of the compressive strength specimens after failure, using the facilities at the Materials Characterization Facility of the Department of Physics and Materials Science, Thapar Institute of Engineering and Technology. The primary aim of this analysis was to identify and characterize the crystalline phases present within the material. In XRD operation, the powdered sample is irradiated with monochromatic X-ray beams, and the diffracted rays are detected and recorded. The resulting diffraction pattern is plotted as intensity versus diffraction angle, producing characteristic peaks that correspond to the atomic structure and crystalline orientation of the phases present. The positions of these peaks indicate the diffraction angles at which constructive interference occurs, while the peak intensities reflect the relative concentration of the associated mineral phases. Each sample from the various concrete mixes was analyzed using a slow scanning procedure across a 2θ range of 10° to 90°, ensuring precise detection of the constituent phases within the cementitious matrix. Scanning Electron Microscopy (SEM) is a microstructural characterization technique used to examine surface morphology and internal features at extremely high magnification.

Figure 3.13 X-ray diffractometer used for the analysis

3.9.2 Scanning Electron Microscope

In concrete analysis, SEM provides valuable insights into microstructural elements such as the cementitious matrix, aggregate interfaces, pore distribution, hydration phases, ettringite formation, and interactions with supplementary cementitious materials. In this study, a Field Emission Scanning Electron Microscope (FE-SEM) was employed, housed at the Materials Characterization Facility of the Department of Physics and Materials Science at Thapar Institute of Engineering and Technology. The specific instrument used was a Zeiss Sigma 500 equipped with Gemini-1 optics. Unlike conventional SEM, FE-SEM utilizes a field emission gun to produce a fine electron beam, resulting in lower image distortion and significantly enhanced resolution. For microstructural analysis, specimens were extracted from the internal core fragments of 100 mm cube samples after compressive strength testing, and these fragments were coated with a thin gold layer prior to imaging to improve conductivity. Additionally, Energy Dispersive Spectroscopy (EDS) was conducted concurrently using the same instrument to obtain elemental composition data. EDS detects characteristic X-ray emissions generated when the electron beam interacts with the sample, enabling elemental mapping and chemical profiling of the concrete microstructure.

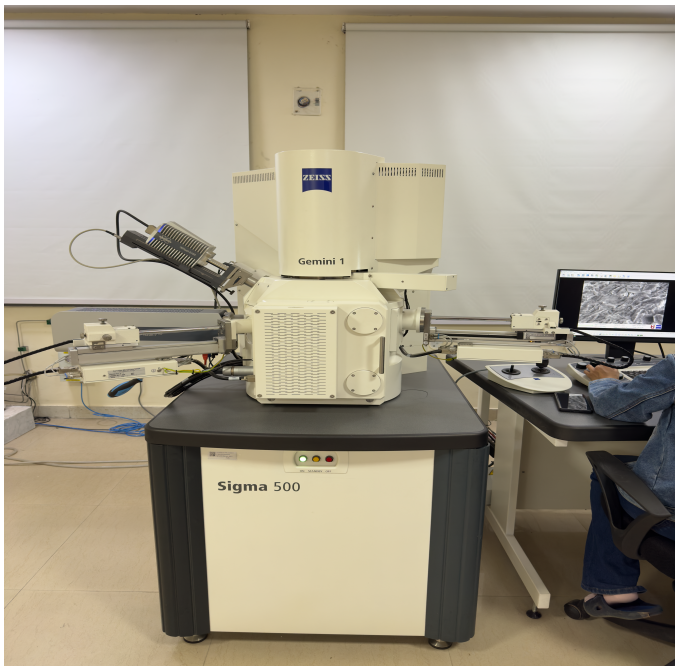

Figure 3.14 Field-emission-Scanning electron microscopy equipment

3.10 Summary

In this chapter, the methodology adopted for the experimental investigation has been presented in a systematic manner, detailing the materials utilized, the preparation and casting procedures, and the various test methods employed to evaluate both fresh and hardened concrete properties. The selection and characterization of materials, along with the standardized testing procedures, ensured reliability and repeatability of results. The prepared mixes were subjected to curing followed by comprehensive mechanical, durability, and microstructural examinations. The following chapter presents and interprets the outcomes of these tests, enabling a thorough analysis of the effects of biochar incorporation on the performance of concrete.

CHAPTER 4
RESULTS AND DISCUSSION

This chapter presents and analyses the experimental results obtained from various tests carried out on the prepared concrete mixes containing different dosages of biochar. The results are structured to sequentially examine: (4.1) the fresh properties of concrete, (4.2) non-destructive evaluation of hardened specimens, (4.3) destructive mechanical strength assessments, (4.4) durability-related performance characteristics of biochar-modified concrete, and (4.5) microstructural analysis and phase characterization of the concrete matrix. Through these data-driven discussions, the performance trends, comparative behaviours, and the influence of biochar incorporation on concrete properties are thoroughly interpreted to support the objectives of the study**.**.

4.1 Fresh state properties

4.1.1 Workability and flow

The slump test was conducted to evaluate the workability and flow behaviour of concrete as a function of increasing biochar content. Throughout all mix proportions, the water–binder ratio and superplasticizer dosage were maintained at constant values of 0.45 and 1% of the binder, respectively, so that any observed changes in fresh properties could be attributed exclusively to the incorporation of biochar. The control mix (0% biochar) exhibited the highest slump diameter, indicating maximum flowability and the least stiffness. With progressive increases in biochar content, the slump diameter gradually decreased, reflecting reduced workability and stiffer mix characteristics. This behaviour is attributed to the strong water absorption and retention capacity of biochar due to its porous and hydrophilic nature, which increases internal moisture demand within the mix. Consequently, higher biochar dosages would likely require additional water or superplasticizer to achieve comparable workability to the control. These findings align with previously published studies by *Jia et al. (2023)* and *Rashid (2025)*, further validating the influence of biochar on fresh concrete behaviour. Results of the slump test are shown in Figure 4.1.

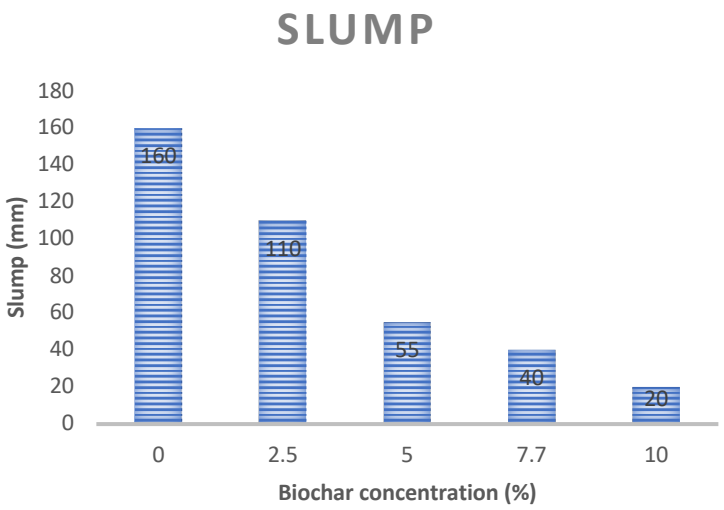

Figure 4.1 Slump-vs-Biochar concentration results

4.2 Non-destructive testing of hardened and cured concrete

4.2.1 Rebound hammer

The rebound hammer test is a non-destructive method used to estimate the compressive strength and assess the surface hardness and uniformity of concrete. The results obtained from this test correspond closely with the findings of the destructive compressive strength tests presented in Section 4.3.1, where mixes M-1, M-2, and M-3 demonstrated progressively higher strength relative to the reference control mix (M-0), with M-3 (containing 7.5% biochar) exhibiting the optimal performance. Mix M-4 showed a reduction in strength compared to M-3, though it still retained improved properties relative to the control. It is important to note that the strength values derived from the rebound hammer tended to be overestimated compared to the destructive compressive strength measurements reported earlier. This discrepancy arises primarily because the rebound number is significantly influenced by the surface hardness characteristics of the specimen, in addition to the intrinsic material integrity and strength of the bulk concrete.

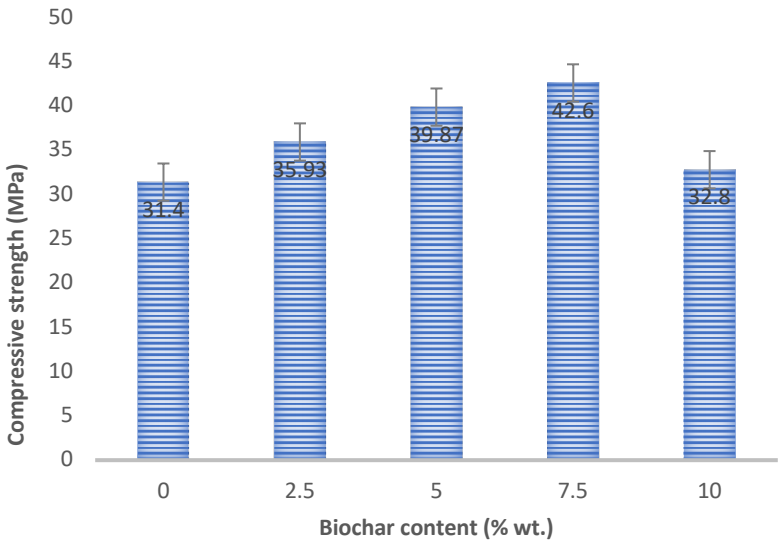

Figure 4.2 Rebound hammer test results at 28 days curing

4.2.2 Ultrasonic pulse velocity

The ultrasonic pulse velocity results obtained at 28 days of curing indicated a clear trend of increasing pulse transmission speed with increasing biochar content up to an optimal replacement level. As biochar dosage increased from 0% to 2.5%, 5%, and 7.5%, the UPV values rose by 0.68%, 2.99%, and 3.63%, respectively, signifying a progressively denser and more homogeneous internal matrix. This trend is consistent with the anticipated micro-filler effect of biochar, where fine particles occupy voids and refine the pore structure. However, this improvement was observed only up to the 7.5% biochar level; beyond this point, at 10% replacement (M-4), the UPV value decreased, indicating increased internal porosity due to excessive incorporation of highly porous biochar particles. Although the UPV of M-4 remained higher than that of the control mix, confirming that filler effects were still present, the diminished velocity compared to M-1 through M-3 suggests that the porosity introduced at higher biochar contents outweighed the densifying benefits. These UPV findings align closely

with the compressive strength results discussed in Section 4.3.1, wherein M-3 (7.5% biochar) exhibited the highest strength among all mixes.

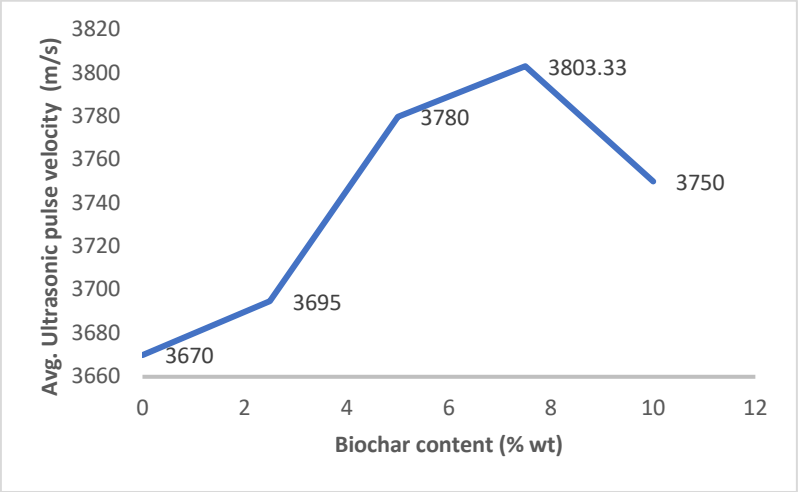

Figure 4.3 Ultrasonic pulse velocity test results at 28 days curing

4.3 Mechanical and strength properties

4.3.1 Compressive strength

The experimental results demonstrated that partial replacement of cement with biochar generally enhanced the compressive strength of concrete, with the exception of the mix containing 10% biochar (M-4). Notably, similar trends of strength gain and subsequent decline with increasing biochar content were observed at both 7-day and 28-day curing ages, indicating consistency in the performance behaviour. At 7 days, the control mix (M-0) exhibited a compressive strength of 19.91 MPa. Incorporation of 2.5% biochar increased this value by 15.87%, while 5% and 7.5% biochar yielded further increases of 23.7% and 30.73%, respectively. This enhancement is attributed to the internal curing capability of biochar, wherein its porous structure absorbs mixing water and gradually releases it during hydration, promoting prolonged hydration and enhanced gel development. However, at 10% biochar dosage, the compressive strength declined by 5.1%, suggesting that the benefit of internal curing was outweighed by excessive porosity.

At 28 days, the compressive strength results further confirmed the optimum performance of M-3 (7.5% biochar), with the control mix (M-0) recording a strength of 28.67 MPa. The

addition of 2.5% biochar resulted in a 12.9% increase, while 5% and 7.5% biochar increased compressive strength by 19.9% and 28.1%, respectively, relative to the control. Conversely, M-4 (10% biochar) exhibited a slight reduction of 1.4% compared to the control. The observed improvement in compressive strength at moderate dosages is consistent with findings reported by *Gupta et al. (2018)*, who attributed the enhancement to the micro-filler activity of biochar, which refines pore structure and densifies the matrix, along with accelerated hydration due to the internal curing effect. The reduction in strength at higher dosage levels is attributed to the dilution of cementitious material and increased void volume introduced by excessive biochar, resulting in the 28-day strength of M-4 being limited to 30.24 MPa.

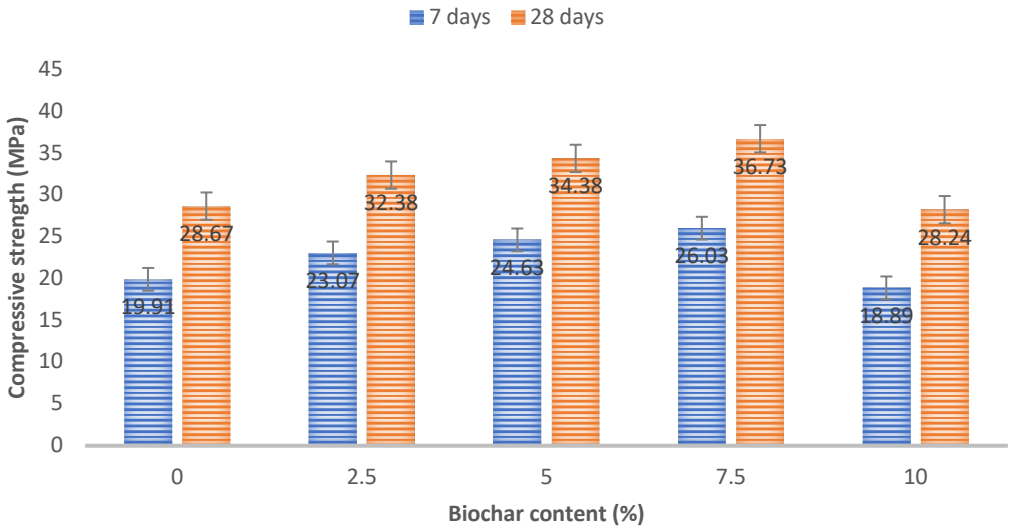

Figure 4.4 Compressive strength test results at different curing ages

4.3.2 Splitting tensile strength

Splitting tensile strength exhibited an overall declining trend with increasing biochar content. At 7 days, the control mix (M-0) demonstrated the highest tensile strength of 1.508 MPa, while the incorporation of biochar led to progressive reductions in tensile capacity. Specifically, dosages of 2.5%, 5%, 7.5%, and 10% biochar resulted in strength decreases of 10.61%, 11.47%, 12.79%, and 31.56%, respectively. A similar pattern was observed at 28 days: the control mix displayed the highest splitting tensile strength of 2.32 MPa, dropping to 2.14 MPa and 2.10 MPa for the 2.5% and 5% mixes. A slight recovery was observed at 7.5% biochar (2.129 MPa), though still lower than the control, followed by a significant reduction to 1.72 MPa at 10% biochar, corresponding to a 25.86% decline. The reduction in tensile performance is primarily attributed to the additional internal porosity introduced by biochar. Owing to its highly porous

structure, biochar creates numerous micropores within the concrete matrix, which can coalesce into larger voids and serve as preferential crack initiation sites under tensile loading. This induces heterogeneity in the matrix, weakens interfacial transition zones, and reduces resistance to tensile stresses. These findings are consistent with results reported by *Gupta et al. (2020)* and *Das et al. (2015),* who similarly noted that biochar-induced porosity negatively affects tensile strength. Furthermore, at higher dosages, the dilution effect reduces the proportion of cementitious material available for hydration, leading to fewer hydration products and consequently lower tensile capacity.

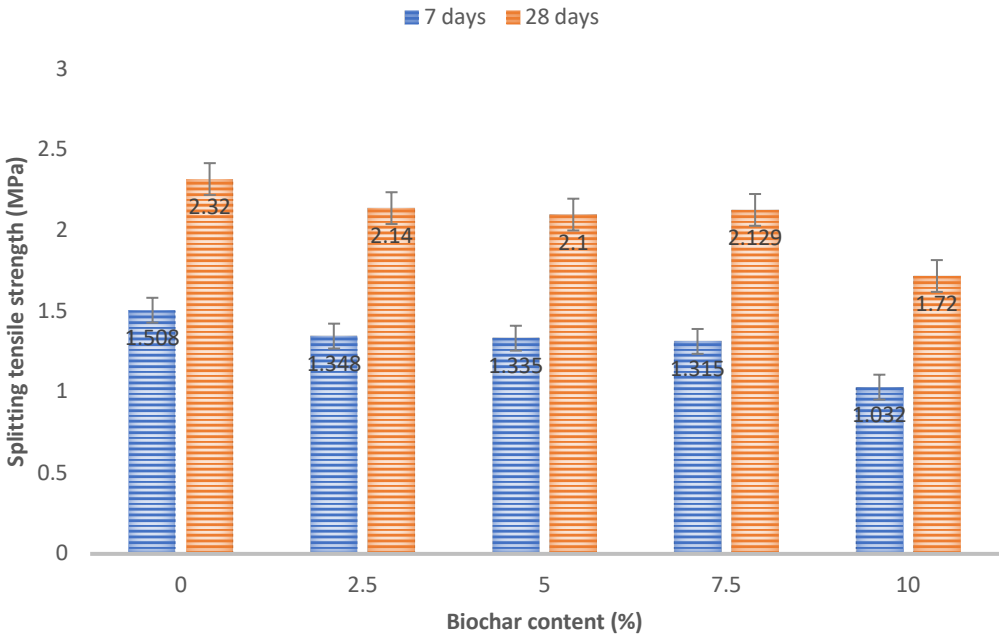

Figure 4.5 Splitting tensile strength test results at different curing ages

4.3.3 Flexural strength

Flexural strength exhibited a decreasing trend with increasing biochar content, similar to the behaviour observed for splitting tensile strength. At 7 days, the highest flexural strength of 3.57 MPa was recorded for the control mix (M-0). With the addition of 2.5%, 5%, 7.5%, and 10% biochar by weight of cement, the corresponding reductions in flexural strength were 1.96%, 10.08%, 11.2%, and 34.73%, respectively. A similar pattern was observed at 28 days, where M-0 exhibited peak flexural strength of 5.336 MPa, while mixes containing 2.5%, 5%, 7.5%, and 10% biochar demonstrated reductions of 6.74%, 11.39%, 11.84%, and 39.5%, respectively. This decline is attributed primarily to the highly porous structure of biochar, which introduces

micro-voids into the matrix, weakening the tensile and bending resistance of the concrete. These micro-voids tend to trap air and promote crack initiation within the tensile zone of the beam, thereby reducing flexural performance a behaviour consistent with the observations of *Gupta and Kua (2019), Rashid et al. (2025),* and *Akhtar and Sarmah (2018)*. Unlike compressive strength, which benefits from matrix densification up to an optimum level, flexural performance is far more sensitive to microstructural discontinuities that support crack propagation, explaining the comparatively sharper reduction in flexural strength with increasing biochar content.

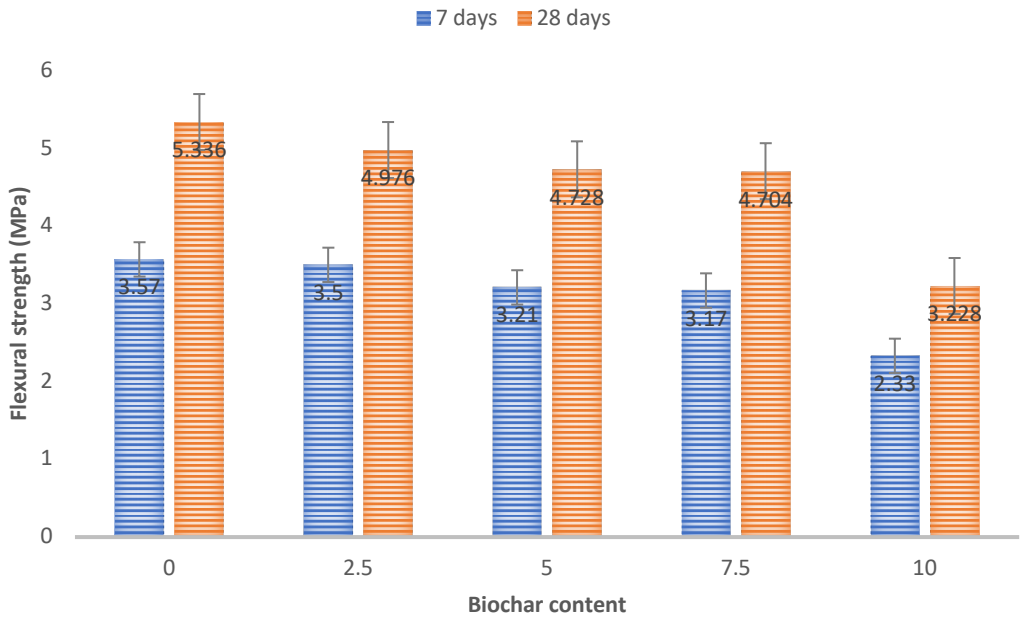

Figure 4.6 Flexural strength test results at different curing ages

4.4 Durability properties

4.4.1 Rapid chloride permeability test

The results of the Rapid Chloride Permeability Test (RCPT) at 28 days revealed a gradual reduction in charge passed from the control mix up to M-2, indicating improved resistance to chloride ion penetration at lower biochar dosages. However, beyond this point, a sharp increase in charge passed was observed for M-3 and more prominently for M-4, reflecting a loss in permeability resistance at higher replacement levels. These findings are consistent with Aman

et al. (2022), who reported that optimal enhancement of chloride resistance occurs at biochar dosages below approximately 6%. The observed performance at lower biochar contents can be attributed to the pore-refinement and micro-filler effects, which reduce capillary pathways and restrict ionic transport. In contrast, higher biochar additions introduce excessive porosity and dilution of the cementitious matrix, thereby increasing permeability and facilitating chloride ingress. The adjusted total charge passed (in Coulombs) for each trial specimen is presented in Figure 4.7, highlighting the comparative changes in chloride permeability across the mixes.

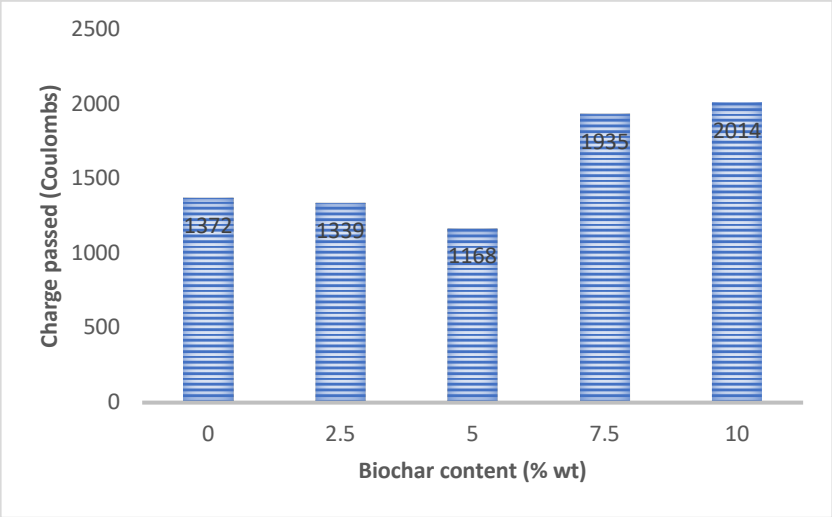

Figure 4.7 Rapid chloride permeability test results at 28 days curing

4.4.2 Water Absorption

The water absorption test conducted at 28 days provided insight into the influence of biochar content on the moisture ingress characteristics and long-term durability of the concrete. The control mix exhibited the lowest water absorption at 4.16%, while water absorption progressively increased with higher biochar dosages, reaching 5.1% for the 10% biochar mix. This trend is attributed to the extremely fine and porous nature of biochar, which introduces additional internal surface area and increases interconnected pore volume within the concrete matrix. Although the micro-filler effect of biochar can enhance compressive strength through internal curing at moderate dosages, its intrinsic porosity simultaneously contributes to a more open pore structure, thereby increasing the material's susceptibility to moisture penetration. These observations are consistent with the findings of *Roy (2017) and Gupta et al. (2020),* who

similarly reported increased water absorption with biochar incorporation due to its strong water affinity and high porosity.

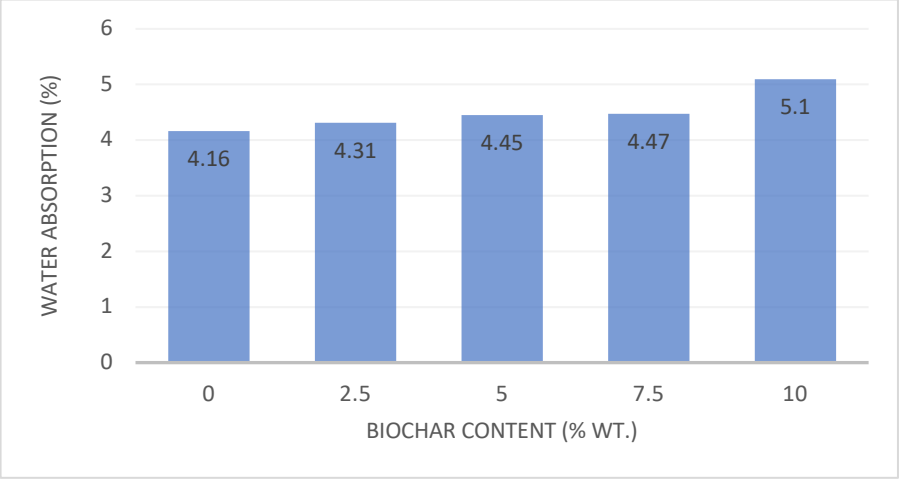

Figure 4.8 Water absorption (%) test results at 28 days curing

4.5 Microstructural analysis and characterization

4.5.1 X-Ray diffraction analysis

The XRD patterns for mixes M0 through M4 (as shown in Figure 4.9) reveal the presence of key crystalline phases typically associated with hydrated cementitious systems. Across all mixes, prominent peaks appear consistently near 2θ values of approximately 26°, 29°, 32–34°, and 50°, which are characteristic signatures of quartz (SiO_2) and calcium silicate hydrate (C–S–H)–related crystalline remnants, along with portlandite formations.

The peak near 26° is associated with quartz originating from the fine aggregate, while the strong signature observed around 29–30° corresponds to calcite and C–S–H hydrates, indicative of the cement hydration process. With the incremental addition of biochar from M1 to M3, there is a modest increase in intensity around the dominant hydration peaks, suggesting improved hydration and the formation of denser binding phases. This enhancement is especially notable in M-3 (7.5% biochar), where the primary hydration peaks showed maximal intensification, reflecting stronger matrix densification and hydration product formation.

However, for M-4 (10% biochar), a slight reduction in peak sharpness and overall peak intensity was observed. This reduction indicates a comparatively less crystalline hydration structure, attributable to the dilution effect and the excessive porosity introduced by higher

biochar content. The slight broadening of peaks suggests an increase in amorphous content and reduced crystalline binding phases.

These XRD observations support the mechanical test results in Section 4.3, wherein M-3 exhibited the highest compressive strength due to optimal densification and hydration, while M-4 showed reduction owing to excessive microstructural porosity.

XRD spectrum of biochar denotes a hump of amorphous, graphitic carbon as expected alongside some impurities.

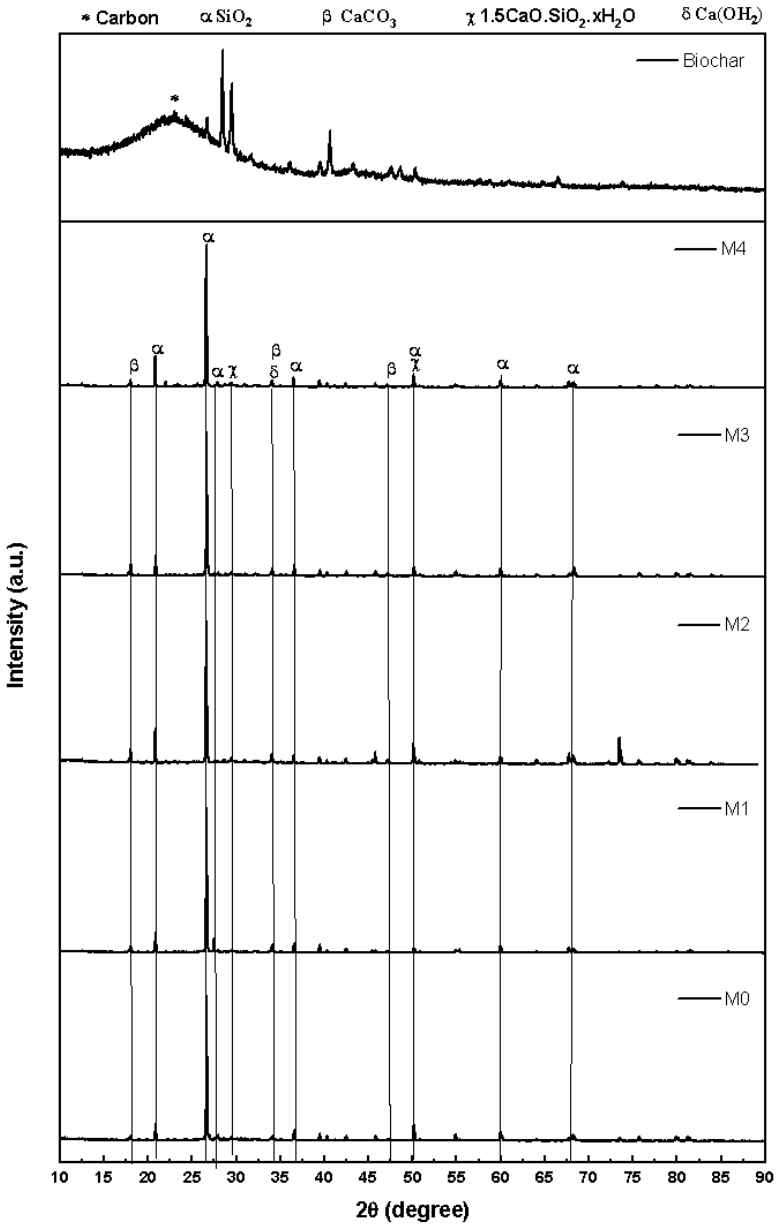

Figure 4.9 X-ray diffraction spectra for different mixes and biochar

4.5.2 Scanning electron microscopy

The SEM microstructural examination revealed a heterogeneous cementitious matrix consisting of well-hydrated calcium-silicate-hydrate (C–S–H) gel formations, embedded aggregate interfaces, and the presence of biochar inclusions distributed within the matrix. The incorporation of biochar appeared to refine the pore morphology at lower dosages, contributing to improved internal compaction through micro-filler behaviour. At higher biochar content, the SEM images indicated increased micropore concentration, illustrating the transition from densification to porosity-dominated microstructure.

Complementing the SEM observations, the EDS spectrum of the sample (as shown in Figure 4.11) identified key elemental constituents typical of hydrated cementitious material. Major detected elements included calcium (Ca), silicon (Si), oxygen (O), aluminium (Al), iron (Fe), magnesium (Mg), potassium (K), and carbon (C). The presence of Ca and Si confirmed the dominance of C–S–H phases which are responsible for compressive strength development. The detected carbon signal further confirms the successful incorporation of biochar within the concrete matrix.

The relatively strong Si and Ca peaks indicate robust hydration and C–S–H presence at optimal replacement levels, while the higher carbon peak intensity at increased biochar dosage is consistent with increased organic phase content and pore formation. The elemental distribution revealed by EDS aligns with the mechanical performance trends discussed earlier in this chapter—namely, increased compressive strength at moderate biochar incorporation followed by strength reduction due to microstructural discontinuity at higher percentages.

Figure 4.10 shows microstructure features such as calcium monosulfate, C-S-H gel, C-S-H gel-Aggregate interface and porous structure of biochar which facilitates as nucleation sites for internal curing effect.

Figure 4.11 shows spectra for different mixes M0 to M4 as represented by (a) to (e), respectively, as obtained from Energy dispersive spectroscopy.

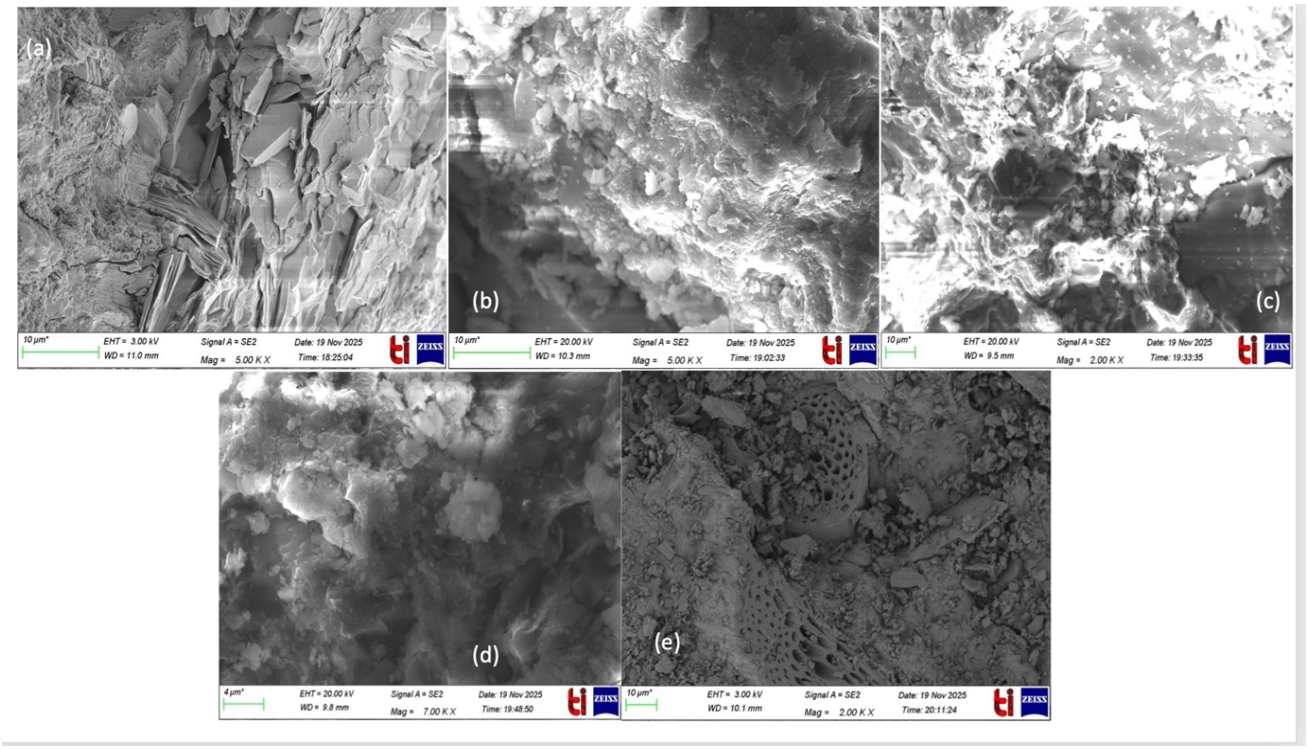

Figure 4.10 Scanning electron micrographs of different mixes

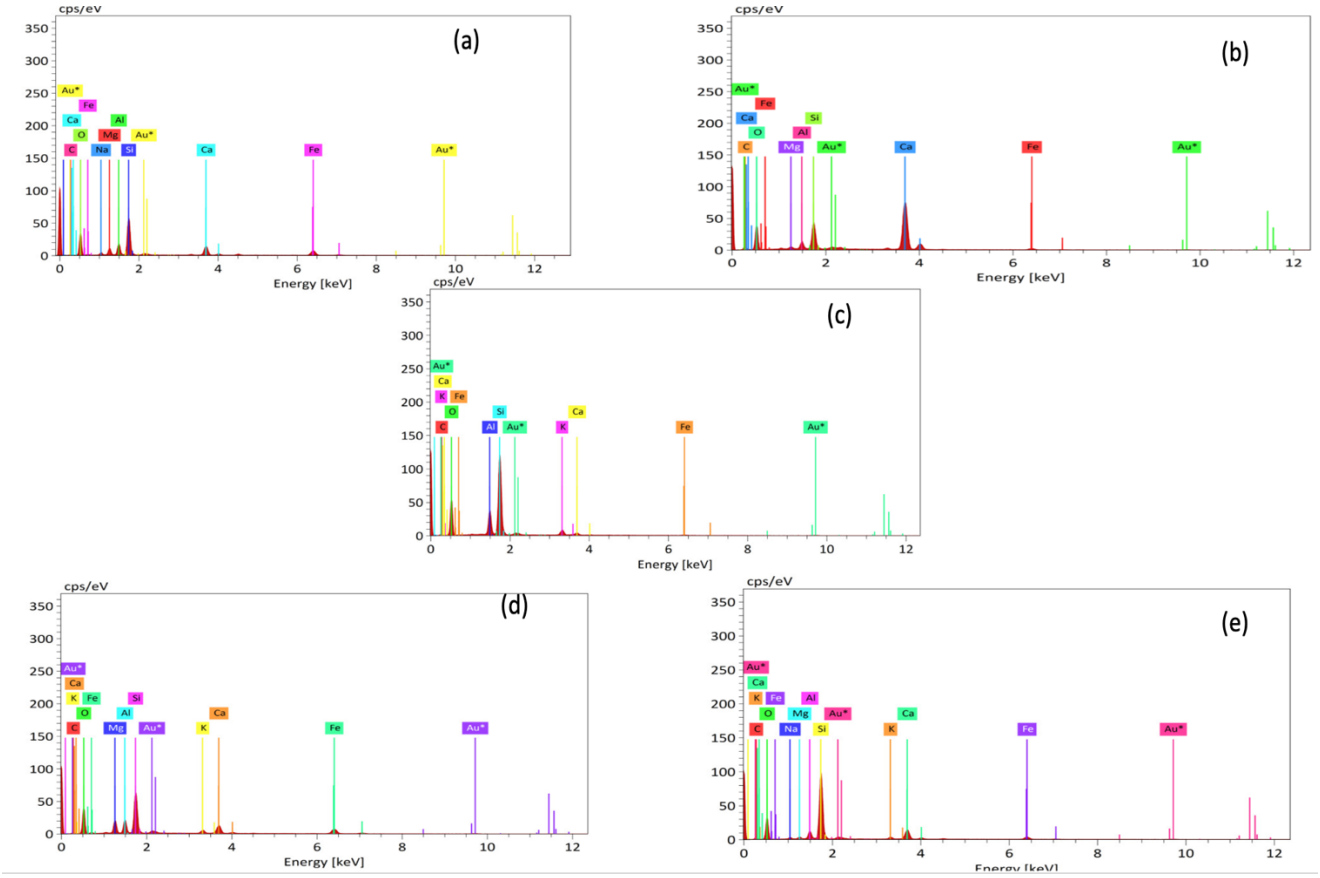

Figure 4.11 Energy dispersive spectra of different mixes

4.6 Summary of Results and Discussion

The results of this investigation clearly demonstrate that the incorporation of biochar as a partial replacement for cement has significant and measurable effects on the fresh, mechanical, durability, and microstructural properties of concrete. Workability assessments showed that slump values decreased with increasing biochar content due to the strong water absorption capacity of biochar, resulting in stiffer mixes at higher replacement levels. Mechanical strength evaluations revealed that compressive strength improved with biochar incorporation up to an optimum dosage of 7.5%, driven by biochar's micro-filler effect and internal curing ability, while both splitting tensile and flexural strengths decreased with increasing biochar content, primarily due to increased micro-porosity and reduced matrix cohesion.

Non-destructive UPV and rebound hammer tests further supported these findings, showing that M-3 (7.5% biochar) achieved the highest density and strength indication, in line with compressive strength performance. Durability indicators presented mixed effects: RCPT results showed reduced chloride permeability at low biochar dosages, followed by a rise at higher dosages due to increased porosity; similarly, water absorption increased progressively with biochar content. Microstructural examinations through FE-SEM and XRD confirmed changes in pore structure and hydration characteristics with increasing biochar content.

Overall, the results indicate that biochar incorporation in concrete is beneficial up to a threshold level of approximately 7.5%, beyond which the adverse effects of excess porosity outweigh the advantages of internal curing and filler contribution. These findings provide valuable insight into the performance of sustainable, carbon-sequestering concrete and guide the optimization of biochar dosage for engineering applications.

CHAPTER 5
CONCLUSIONS AND SUMMARY

This study established that the incorporation of biochar as a partial replacement for Ordinary Portland Cement has a significant and generally positive influence on the performance of concrete. The most notable improvement was observed in the compressive strength, which consistently increased with biochar addition up to an optimal dosage of 7.5% (M-3). This enhancement is primarily attributed to the micro-filler effect, whereby the fine biochar particles occupy micro-void spaces within the matrix, leading to a denser and more refined pore structure. Even at 10% dosage, the compressive strength remained higher than that of the control mix, though slightly lower than the optimal 7.5% replacement.

- The rebound hammer test results supported these findings, demonstrating similar performance trends. However, rebound-based compressive strength values were somewhat overestimated due to dependence on superficial surface hardness, which does not always fully represent the integrity of the material bulk.
- Ultrasonic Pulse Velocity (UPV) measurements further corroborated the mechanical test outcomes, showing increasing pulse velocity with higher biochar content up to 7.5%, indicating improved internal uniformity and density. At 10% dosage, the UPV value declined slightly, yet remained higher than that of the control mix, demonstrating that filler-driven densification persisted, though partially offset by porosity.
- Biochar's contribution to performance enhancement is rooted in its high surface area, internal pore structure, and ability to participate in pozzolanic interactions. These characteristics enable biochar to function as a localized internal curing agent, absorbing water and CO_2 during mixing and gradually releasing them to sustain extended hydration. In this manner, biochar pore networks serve as nucleation sites for hydration products, promoting microstructural development.
- Workability results showed a consistent reduction in slump with increasing biochar content, reflecting the high water demand induced by biochar due to its absorption-driven self-desiccation effect. With constant water content and constant superplasticizer dosage, higher biochar mixes behaved more stiffly compared to lower replacement mixes or the control, indicating reduced flowability.

The findings demonstrate that the performance of biochar-modified concrete depends critically on dosage. At lower concentrations (≤7.5%), biochar enhances matrix density, hydration, and compressive strength. However, excessive replacement beyond this threshold introduces surplus porosity, increasing void connectivity and impairing tensile-driven strength parameters. As a result, splitting tensile strength and flexural strength showed consistent declines at all biochar dosages due to crack-initiating voids formed especially in tensile stress regions. Overall, the study confirms that biochar exhibits strong potential as an effective, sustainable cement-replacement material, with a verified optimum content of approximately 7.5% for maximizing compressive performance while maintaining structural reliability.

FUTURE SCOPE

Future studies should evaluate the mechanical and durability behaviour of biochar-modified concrete over extended curing periods, such as 56, 90, and 180 days, to assess the long-term performance and stability of hydration-derived phases. Beyond the tests conducted in this research, there is also substantial potential for expanding the experimental program to incorporate additional durability assessments, including freeze thaw resistance, sulphate attack, carbonation depth, oxygen permeability, and thermal degradation resistance.

Since CO_2 sequestration remains one of the most significant environmental benefits of biochar incorporation, long-term life-cycle assessments (LCA) and embodied emissions analysis should be undertaken to quantitatively determine the net carbon reduction impact of biochar concrete across its service life. Additionally, existing literature suggests that chemically treated or functionalized biochar often produces superior performance enhancements compared to untreated biochar; therefore, further exploration of chemically modified biochar and its influence on hydration, pore structure, and performance is warranted.

There also exists strong research potential in conducting comparative studies on cementitious composites utilizing biochar derived from different feedstock sources, as biochar produced from varying biomass types differs significantly in mineral composition and pore morphology. Similarly, the effects of pyrolysis temperature should be systematically investigated, as thermal parameters directly influence biochar surface area, porosity, and carbon structure. Furthermore, comparative evaluations of biochar subjected to different physical processing methods—including grinding, milling, or particle-size modification should be undertaken to understand how particle morphology influences binder hydration, matrix densification, and mechanical behavior.

REFERENCES

(1) Habert, G., Miller, S.A., John, V.M., Provis. J.L, Favier, A., Horvath, A., Scrivener, K.L., (2020). Environmental impacts and decarbonization strategies in the cement and concrete industries, Nature Reviews Earth and Environment 1: 559-57

(2) Johannes Lehmann, Annette Cowie, Caroline A. Masiello, Claudia Kammann, Dominic Woolf, James E. Amonette, Maria L. Cayuela, Marta Camps-Arbestain, Thea Whitman (2021). Biochar in climate change mitigation, Nature Geoscience 14: 883-892

(3) Maljaee, H., Madadi R., Paiva H. (2021). Incorporation of biochar in cementitious materials: a roadmap of biochar selection. Construction and Building Materials 283:122757

(4) Windeatt, J.H., Ross, A.B., Williams, P.T., Forster P.M., Nahil, M.A., Singh, S. (2014) Characteristics of biochars from crop residues: potential for carbon sequestration and soil amendment. Journal of Environmental Management 146:189-197

(5) Gupta, S., Kua, H.W., Low, C.Y. (2018). Use of biochar as carbon sequestering additive in cement mortar, Cement and Concrete Composites 87:110-129.

(6) Sourabdeep Gupta, Padmaja Krishnan, Alireza Kashani, Harn Wei, Kua (2020). Application of biochar from coconut and wood waste to reduce shrinkage and improve physical properties of silica fume-cement mortar, Construction and Building Materials 262: 120688

(7) Liu, W., Li, K., Xu, S. (2022). Utilizing bamboo biochar in cement mortar as a bio-modifier to improve the compressive strength and crack-resistance fracture ability, Construction and Building Materials 327:126917

(8) Roy, K., Akhtar, A., Sachdev, S.D., Hsu, M., Lim, J.B.P., Sarmah, A., (2017). Development and characterization of novel biochar-mortar composite utilizing waste derived pyrolysis biochar, International Journal of Scientific and Engineering Research, Volume 8, Issue 12

(9) Jia, Y., Li, H., Xiaole He, Li, P., Wang Z. (2023). Effect of biochar from municipal solid waste on mechanical and freeze–thaw properties of concrete, Construction and Building Materials 368:130374

(10) Zeidabadi, Z.A., Bakhtiari, S., Abbaslou, H., Ghanizadeh, A.L. (2018). Synthesis, characterization and evaluation of biochar from agricultural waste biomass for use in building materials, Construction and Building Materials 181:301-308

(11) Du, J., Wang, Y., Bao, Y., Sarkar, D., Meng, W. (2023). Valorization of wasted-derived biochar in ultra-high-performance concrete (UHPC): pretreatment, characterization, and environmental benefits, Construction and Building Materials 409:133839

(12) Ling, Y., Wu Xionghua, Tan, K., Zou, Z. (2023). Effect of Biochar Dosage and Fineness on the Mechanical Properties and Durability of Concrete, Materials 2023, 16, 2809

(13) Tang, Y., Qiu, J. (2024). CO_2-sequestering ability of lightweight concrete based on reactive magnesia cement and high-dosage biochar aggregate, Journal of Cleaner Production 451: 141922

(14) Praneeth, S., Saavedra, L., Zeng, M., Dubey, B.K., Sarmah, A.K. (2021). Biochar admixtured lightweight, porous and tougher cement mortars: Mechanical, durability and micro computed tomography analysis, Science of the Total Environment 750: 142327

(15) Zhang, Q., Dong, S., Wu, F., Cai, Y., Xie, L., Huang, C., Zhao, J., Yang, S., Xu, F., Zhu, Z., Luo, P. (2024). Investigation of the macro performance and mechanism of biochar modified ultra-high performance concrete, Case Studies in Construction Materials 21: e03595

(16) Maljaee, H., Rozita M., Paiva H., Tarelho, L., Morais, M., Ferreira, V.M. (2022). Sustainable lightweight mortar using biochar as sand replacement, European Journal of Environmental and Civil Engineering, Taylor and Francis, 2022, VOL. 26, No. 16, 8263-8279

(17) Wyrzykowski, M., Toropovs, N., Winnefeld, F., Lura, P. (2024). Cold-bonded biochar-rich lightweight aggregates for net-zero concrete, Journal of Cleaner Production 434: 140008

(18) Sharma, R.K., Lakhani, R. (2023). Microstructural and Thermo- mechanical Properties of Energy- Efficient Structural Lightweight Concrete with LECA, Fly ash and Marble slurry, Proceedings on Innovative and Sustainable Materials and Technology

(19) Zou, S., Lu, Jian-Xin, Xiao, J., Duan, Z., Chau, C.K., Sham, M.L., Poon, C.S. (2023). Development and characteristics of novel high-strength lightweight core-shell aggregate, Construction and Building Materials 393: 132080

(20) Sirico, A., Bernardi. P., Sciancalepore, C., Vecchi, F., Malcevschi, A., Belletti, B., Milanese, D. (2021). Biochar from wood waste as additive for structural concrete, Construction and Building Materials 303: 124500

(21) Chen, L., Zhu, X., Zheng, Y., Wang, L., Poon, C.S., Tsang, Daniel C.W. (2024). Development of high-strength lightweight concrete by utilizing food waste digestate based biochar aggregate. Construction and Building Materials 411: 134142

(22) Gupta, S., Kua, H.W. (2020). Application of rice husk biochar as filler in cenosphere modified mortar: Preparation, characterization and performance under elevated temperature. Construction and Building Materials 253: 119083

(23) Castillo, E.D.R., Almesfer, N., Saggi, O., Ingham, J.M. (2020). Light-weight concrete with artificial aggregate manufactured from plastic waste. Construction and Building Materials 265: 120199

(24) Javed, M.H., Sikander, M.A., Ahmad, W., Bashir, M.T., Alrowais, R., Wadud M.B. (2022). Effect of various biochars on physical, mechanical, and microstructural characteristics of cement pastes and mortars. Journal of Building Engineering 57:104850

(25) Danish, A., Mosaberpanah, M.A., Salim, M.U., Ahmad, N., Ahmad, F., Ahmad, A. (2021). Reusing biochar as a filler or cement replacement material in cementitious composites: A review. Construction and Building Materials 300: 124295

(26) Lu, Jian-Xin. (2023). Recent advances in high strength lightweight concrete: From development

strategies to practical applications. Construction and Building Materials 400:132905

(27) Senadheera, S.S., Gupta, S., Kua, H.W., Hou, D., Kim, S., Tsang, D., Ok, Y.S. (2023). Application of biochar in concrete – A review. Cement and Concrete Composites 143: 105204

(28) Tayyab, S., Ferdous, W., Lokuge, W., Siddique, R., Manalo, A. (2024). Biochar in cementitious composites: A comprehensive review of properties, compatibility, and prospect of use in sustainable geopolymer concrete. Resources, Conservation and Recycling Advances.

(29) Liu, J., Liu, G., Zhang, W., Li, Z., Jin, H., Xing, F. (2023). A new approach to CO_2 capture and sequestration: A novel carbon capture artificial aggregates made from biochar and municipal waste incineration bottom ash. Construction and Building Materials 398: 132472

(30) Roychand, R., Lynch, S.K., Saberian, M., Li, J., Zhang, G., Li, C.Q. (2023). Transforming spent coffee grounds into a valuable resource for the enhancement of concrete strength. Journal of Cleaner Production 419: 138205

(31) Sirico, A., Belletti, B., Bernardi, P., Malcevschi, A., Pagliari, F., Fornomi, P., Moretti, E. (2022). Effects of biochar addition on long-term behavior of concrete. Theoretical and Applied Fracture Mechanics 122: 103626

(32) Zou, S., Sham, M.L., Xiao, J., Leung, L.M., Lu, Jian-Xin, Poon, C.S. (2024). Biochar-enabled carbon negative aggregate designed by core-shell structure: A novel biochar utilizing method in concrete. Construction and Building Materials 449:138507

(33) Sharma, R.K., Srivastava, A. (2022). Influence of Lightweight Aggregates and Supplementary Cementitious Materials on the Properties of Lightweight Aggregate Concretes. Iranian Journal of Science and Technology 935: 27

(34) Agarwal, R., Pawar, N., Supriya, Rawat, P., Rai, D., Kumar, R., Naik, S.B. (2023). Thermo-mechanical behavior of cementitious material with partial replacement of Class-II biochar with Accelerated Carbonation Curing (ACC). Industrial Crops and Products 204: 117335

(35) Yamamoto, S., Yukita, K., Tanaka, H., Kubo, M., Shimizu, K. (2024). Versatility and decarbonizing effect of concrete mixed with biochar. Proceedings of the Sixth International Conference on Sustainable materials and Technologies.

(36) Roy, K., Lim, J.B.P., Sarmah, A.K. (2017). Development and characterization of novel biochar-mortar composite utilizing waste derived pyrolysis biochar. International Journal of Scientific and Engineering Research Volume 8, Issue 12

(37) Mishra, G., Danoglidis, P., Shah, S.P., Gdoutos, M.K. (2023). Optimization of biochar and fly ash to improve mechanical properties and CO_2 sequestration in cement mortar. Construction and Building Materials 392: 132021

(38) Ahmad, S., Khushnood, R.A., Jagdale, P., Tulliani, J.M., Ferro, G.A. (2015). High performance self-consolidating cementitious composites by using micro carbonized bamboo particles. Materials and Design 76: 223-229

(39) Gupta, S., Kua, H.W. (2018). Effect of water entrainment by pre-soaked biochar particles on strength and permeability of cement mortar. Construction and Building Materials 159: 107-125

(40) Rodier, L., Bilba, K., Onésippe, C., Arsène, M.A. (2019). Utilization of bio-chars from sugarcane bagasse pyrolysis in cement-based composites. Industrial Crops and Products, Vol 141

(41) Rashid, Sarmad; Goyal, Arpit; Roy, Danie A.B.; Singh Manpreet (2026). Effect of Physical Modification of Biochar on its Characteristics and Cementitious properties. Journal of Materials in Civil Engineering 2026, 38(2): 04025534

(41) Aneja, Akash; Sharma, R.L.; Singh, Harpal (2022). Mechanical and durability properties of biochar concrete. Materials Today: Proceedings 65 (2022) 3724-3730

(42) Rashid, Sarmad; Goyal, Arpit; Roy, Danie A.B.; Singh Manpreet (2025). Synergistic effect of physical modification and accelerated carbonation curing on the cementitious properties and

carbon sequestration potential of biochar cement composites. Journal of Sustainable Cement-based Materials 2165-0373

(43) Rashid, Sarmad; Raghav, Abhishek; Goyal, Arpit; Roy, Danie A.B.; Singh Manpreet (2024). Biochar as a sustainable additive in cementitious composites: A comprehensive analysis of properties and environmental impact. Industrial Crops and Products 209 (2024) 118044

(44) Rashid, Sarmad; Goyal, Arpit; Roy, Danie A.B.; Singh Manpreet (2025). Application of stubble waste biochar in cementitious composites: the impact of pyrolysis temperature on its characteristics and cementitious performance. Waste Management 206 (2025) 115088

(45) Aman, Aan Mohammed Nusrat; Selvarajoo, Anurita; Lau, Teck Leong; Chen, Wei-Hsin (2022). Biochar as cement replacement to enhance concrete composite properties: A reivew. Energies 2022, 15, 7662.

EVALUATION OF STRENGTH AND DURABILITY PROPERTIES OF CEMENTITIOUS COMPOSITES WITH RICE STUBBLE BIOCHAR AS PARTIAL BINDER REPLACEMENT

ORIGINALITY REPORT

19%	11%	17%	5%
SIMILARITY INDEX	INTERNET SOURCES	PUBLICATIONS	STUDENT PAPERS

PRIMARY SOURCES

1	Souradeep Gupta, Padmaja Krishnan, Alireza Kashani, Harn Wei Kua. "Application of biochar from coconut and wood waste to reduce shrinkage and improve physical properties of silica fume-cement mortar", Construction and Building Materials, 2020 Publication	1%
2	Sai Praneeth, Laureen Saavedra, Maria Zeng, Brajesh K. Dubey, Ajit K. Sarmah. "Biochar admixtured lightweight, porous and tougher cement mortars: Mechanical, durability and micro computed tomography analysis", Science of The Total Environment, 2020 Publication	1%
3	Mateusz Wyrzykowski, Nikolajs Toropovs, Frank Winnefeld, Pietro Lura. "Cold-bonded biochar-rich lightweight aggregates for net-zero concrete", Journal of Cleaner Production, 2024 Publication	1%
4	Qiuyue Zhang, Shuangkuai Dong, Fufei Wu, Yang Cai et al. "Investigation of the macro performance and mechanism of biochar modified ultra-high performance concrete", Case Studies in Construction Materials, 2024 Publication	1%

5	Internet Source	1 %
6	ebin.pub Internet Source	1 %
7	www.researchgate.net Internet Source	1 %
8	Alice Sirico, Patrizia Bernardi, Corrado Sciancalepore, Francesca Vecchi et al. "Biochar from wood waste as additive for structural concrete", Construction and Building Materials, 2021 Publication	<1 %
9	naac.gcoen.ac.in Internet Source	<1 %
10	Hamid Maljaee, Rozita Madadi, Helena Paiva, Luís Tarelho, Miguel Morais, Victor M. Ferreira. "Sustainable lightweight mortar using biochar as sand replacement", European Journal of Environmental and Civil Engineering, 2021 Publication	<1 %
11	Rajeev Roychand, Savankumar Patel, Pobitra Halder, Sazal Kundu et al. "Recycling biosolids as cement composites in raw, pyrolysed and ashed forms: a waste utilisation approach to support circular economy", Journal of Building Engineering, 2021 Publication	<1 %
12	"Sustainable Construction and Building Materials", Springer Science and Business Media LLC, 2019 Publication	<1 %
13	dspace.thapar.edu:8080 Internet Source	<1 %